

1-1-1997

Characterization of variable molecular weight and alternative solvent poly(methylmethacrylate) resist systems for electron beam lithography

Todd Eakin

Follow this and additional works at: <http://scholarworks.rit.edu/theses>

Recommended Citation

Eakin, Todd, "Characterization of variable molecular weight and alternative solvent poly(methylmethacrylate) resist systems for electron beam lithography" (1997). Thesis. Rochester Institute of Technology. Accessed from

This Thesis is brought to you for free and open access by the Thesis/Dissertation Collections at RIT Scholar Works. It has been accepted for inclusion in Theses by an authorized administrator of RIT Scholar Works. For more information, please contact ritscholarworks@rit.edu.

**CHARACTERIZATION OF VARIABLE MOLECULAR
WEIGHT AND ALTERNATIVE SOLVENT
POLY(METHYLMETHACRYLATE) RESIST SYSTEMS
FOR ELECTRON BEAM LITHOGRAPHY**

Todd Eakin

**THESIS
SESM-879
MATERIALS SCIENCE & ENGINEERING
ROCHESTER INSTITUTE OF TECHNOLOGY**

Bruce Smith, Professor of Microelectronics

Robert Clark, Dean, College of Science

John Arney, Professor of Imaging Science

LIBRARY RELEASE

I, Todd Eakin, hereby grant permission to the Wallace Library of the Rochester Institute of Technology to maintain a copy and to reproduce my thesis in whole or in part. Any reproduction will not be for commercial use or profit.

Todd Eakin

CHARACTERIZATION OF VARIABLE MOLECULAR WEIGHT AND ALTERNATIVE SOLVENT POLY(METHYLMETHACRYLATE) RESIST SYSTEMS FOR ELECTRON BEAM LITHOGRAPHY

ABSTRACT

Poly(methylmethacrylate), PMMA, resist samples with varying weight average molecular weights and several non-chlorobenzene casting solvents were characterized utilizing electron beam lithography. Environmental concerns with chlorobenzene have motivated investigation into alternative casting solvents for PMMA resists. Processing effects of variation in the molecular weight of the PMMA resin were unknown and have been quantified. Weight average molecular weights ranging from 539,000 g/mol to 614,000 g/mol were studied in chlorobenzene resist systems. Chlorobenzene, anisole, butyl-acetate, and propylene glycol monoethyl ether acetate solvents were studied in resist systems of constant weight average molecular weight. A three stage screening, optimization, and confirmation experiment was conducted to characterize the different experimental PMMA resist systems. Pre-bake temperature was the only processing input factor to be affected by solvent type. Weight average molecular weight had no statistically significant effect in performance of any resist sample. Measured performance outputs, patterned linewidth, did not significantly vary between the experimental samples. The solvents, chlorobenzene, anisole, and propylene glycol monoethyl ether acetate, and weight average molecular weights ranging from 539,000 g/mol to 614,000 g/mol gave equivalent performance in PMMA resist systems.

**CHARACTERIZATION OF VARIABLE MOLECULAR
WEIGHT AND ALTERNATIVE SOLVENT
POLY(METHYLMETHACRYLATE) RESIST SYSTEMS
FOR ELECTRON BEAM LITHOGRAPHY**

Todd Eakin

Table of Contents

Introduction	1
Background of PMMA Resists	1
Alternatives for PMMA Resists	2
Theory	5
Electron Beam Lithography	5
PMMA Radiation Chemistry	11
Experiment	17
Results and Discussion	23
Screening Experiment	23
Optimization Experiment	27
Confirmation Runs	35
Conclusions	37
References	39
Appendices	41

FIGURES AND TABLES

Figure 1.	Electron Beam Lithography System.	5
Figure 2.	Interaction of electron beam encountering a solid.	6
Figure 3.	Simulated trajectories of electrons in a PMMA film on Si .	10
Figure 4.	Schematic of decomposition paths for PMMA.	11
Figure 5.	Line and space test pattern used for sample patterning.	21
Figure 6.	Spin speed coating characteristic curves of samples studied.	23
Figure 7.	Evaporation rate for experimental solvents.	26
Figure 8.	T-tests of contrast for each experimental solvent & M_w .	27
Figure 9.	Midpoint contrast curves, bordered by high & low E_0 , curves.	28
Figure 10.	T-test of Dose to Clear (E_0) for each experimental sample.	29
Figure 11.	Normal probability plots for responses contrast and E_0 .	30
Figure 12.	Effect plots of responses to input factors.	31
Figure 13.	Summary contour plots for responses contrast and E_0 .	32
Figure 14.	Plot of measured linewidth versus exposure dose.	33
Figure 15.	Effect of dispersity, M_w and dose on linewidth.	35
Figure 16.	T-test of linewidth for each experimental solvent.	36
Table 1.	Solubility parameters for experimental casting solvents.	13
Table 2.	Solubility principal force and develop parameters.	14
Table 3.	PMMA resist systems used in experiment.	17
Table 4.	Steps for wafer cleaning process.	18
Table 5.	Conditions for experimental optimization.	20
Table 6.	Calculated spin speeds for experimental samples.	24
Table 7.	Grouped sample evaporation rates.	25
Table 8.	Optimal input factors calculated from contour plots.	32
Table 9.	Optimal input factors calculated from experimental analysis.	34
Table 10.	Optimal input factors with summary experimental results.	37

INTRODUCTION

Poly(methylmethacrylate), PMMA, is used as a positive tone electron beam resist. PMMA's functionality as a high resolution electron beam resist was demonstrated by Hatzakis in 1969 [1]. PMMA resin is cast in a carrier solvent to form a resist solution which can be applied to a substrate.

Regions of the PMMA are made more soluble by exposure to electron beam radiation. Developer solvents are then used to differentially dissolve away the exposed areas. Over the years, these basic processes have been used to apply PMMA in many different areas in the microelectronic industry.

However, due to regulatory constraints on casting solvents and variation in the manufacture of resins, PMMA must be re-characterized to insure it's continued use in the microelectronic industry.

Background of PMMA Resists

PMMA is used in a wide variety of lithographic applications. The flexibility of electron beam exposure systems, by directing the electron beam to expose specific regions, enhances the functionality of PMMA as an electron beam resist. Maskmaking is one area of application for PMMA resists. PMMA exhibits consistent day-to-day performance which is a key factor for maskmaking applications. Repeatable performance and available high resolution make PMMA attractive for use in typical and special-case maskmaking applications. PMMA resists can also be utilized in direct, electron beam write-on-wafer applications. The high resolution qualities of PMMA can be combined with the flexibility of electron beam lithography to

produce direct write, fine featured devices [2]. The primary use for PMMA resist systems is in specialized segments of microelectronic lithography such as T-Gate fabrication. PMMA resists paired with electron beam lithography are well suited for T-Gate fabrication [3]. T-Gate fabrication utilizes a dual-layer resist scheme to manufacture high speed devices. High resolution PMMA and a lower resolution co-polymer such as P[MMA-co-MAA] absorb direct electron beam radiation to produce T shaped structures. T shaped devices utilize a narrow gate portion for high switching speeds while the top of the gate is wider for high transconductance in field effect transistors. Specialized segments of microelectronic industry such as T-Gate fabrication, operate with a low volume and high part count. Electron beam lithography and PMMA resist system provide the needed versatility to make these applications successful.

PMMA has the advantage of still being considered one of the highest resolution materials available [4]. PMMA can be patterned with features ranging in dimension from several microns to well below the sub-0.25 μm range when used in electron beam lithographic applications. The wide processing range of resolution and processing stability are key features for PMMA. High resolution has extended the life of PMMA for the highly specialized microelectronic e-beam applications.

Alternatives for PMMA Resists

There are two major elements in PMMA resist systems that restrict it's ease of integration in today's manufacturing processes. First, the casting solvent, chlorobenzene, limits the extent to which PMMA can be used

throughout the microelectronic industry. Chlorobenzene is toxic and poses a health hazard. The Material Safety Data Sheet located in Appendix A details the detrimental affects of chlorobenzene. The unfavorable properties of chlorobenzene include flammability and neuro-toxicity. Chlorobenzene evolves hazardous by-products, inhalation of 200 ppm causes eye and nasal irritation, and exposure to 2400 ppm is immediately dangerous to life and health. Processing and disposal of solvents such as chlorobenzene are also becoming a costly procedure. With a raised awareness for the environment, the cost of using chlorobenzene is becoming very high in order to avoid it's potentially hazardous effects. The second major area of concern is molecular weight. PMMA is produced with general high volume applications in mind, such as commercial plastics. It is not typically manufactured with the quality and control needed for specialty microelectronic applications. The variations in the incoming material may adversely affect performance of the PMMA resist system. Resolution could suffer and variations in processing could have a negative economic impact for the user.

The focus of this work is two-fold; evaluate performance of non-chlorobenzene casting solvents, and evaluate PMMA resist system performance across a range of weight average molecular weights (M_w). Chlorobenzene exhibits desirable characteristics, giving low viscosity solutions, resist systems with low percent solids and it does not interfere in subsequent processing stages. Other solvents must be found to cast the methacrylate resin. Propylene glycol monoethyl ether acetate (PGMEA),

anisole, and butyl-acetate are a few possibilities. These are safer, more environmentally acceptable, solvents. They will be tested to evaluate their performance as casting solvents in place of chlorobenzene.

For consistent processing, a repeatable batch to batch molecular weight is desired. Changes in molecular weight can effect several processing parameters such as, dose to clear, development, and resolution. However, the range of tolerable molecular weight variation needs to be quantified.

PMMA resist formulations at several molecular weights cast in chlorobenzene will be evaluated to quantify the effect molecular weight has on lithographic performance.

THEORY

Electron Beam Lithography

Electron beam lithography has evolved from primitive systems with a manually controlled beam to automated high speed scanning computer controlled lithography systems. The first electron beam lithography was performed in a SEM (Scanning Electron Microscope) system. Here the beam was manually controlled to create simple patterns in resist. Current electron beam lithography systems are much more automated. A basic configuration is shown (Figure 1). A computer operates the electrostatic and magnetic beam controls while commanding the X-Y stage. Resist exposure is controlled by the speed at which the electron beam and stage are moved. Pattern generation is automatically controlled by a computer.

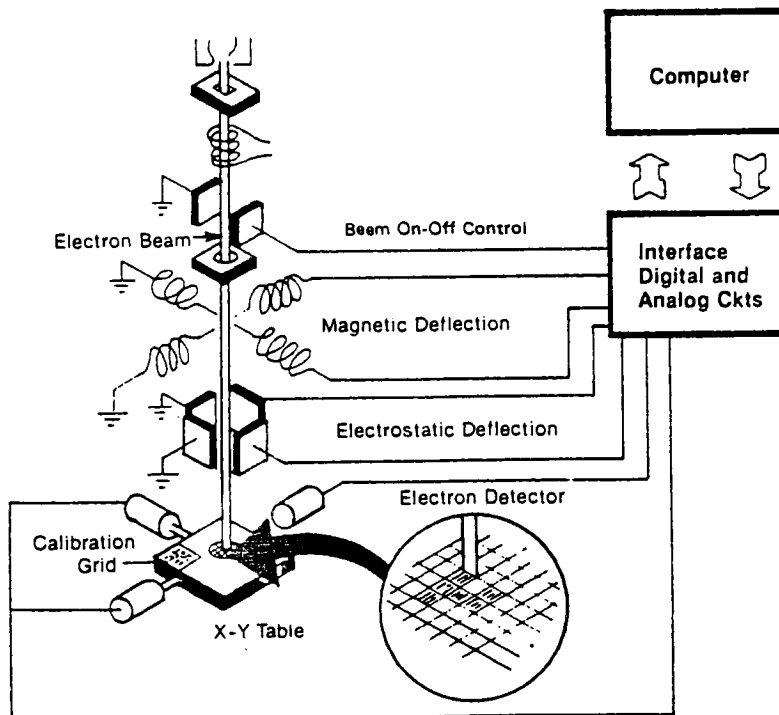


Figure 1. Electron Beam Lithography System [5].

The interaction of an electron beam in a solid is an important aspect of electron beam lithography. Backscattered electrons, absorbed electrons, secondary electrons, and characteristic x-rays, result from an area within the solid irradiated by an electron beam. Figure 2 illustrates the number of different process that occur when an electron beam strikes a solid.

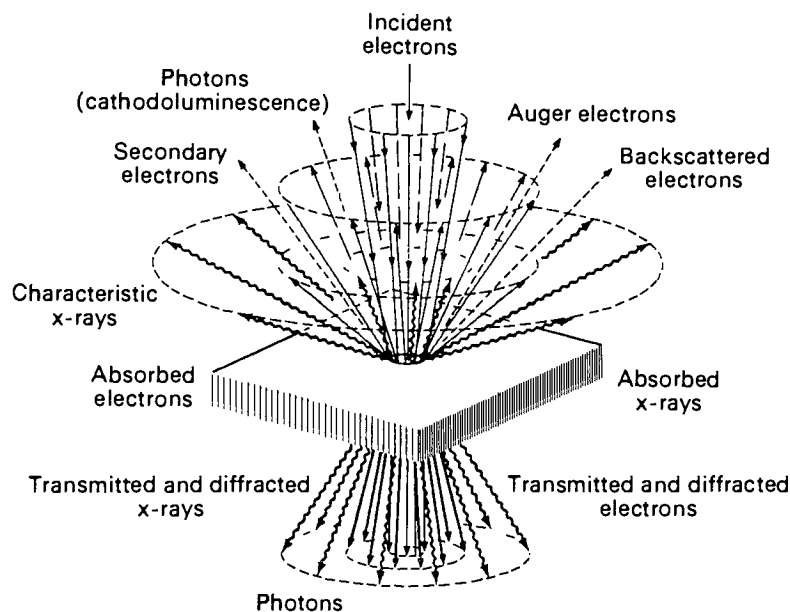


Figure 2. Interaction of electron beam encountering a solid [6].

When the electron beam enters a solid, interactive scattering processes cause beam spreading. As the electron beam propagates into the material, the beam spreading results in lateral dispersion. Consequently, there is an enlargement of the volume in which ionization occurs. Essentially there are three modes of electron beam interactions within solid materials. These are absorption, elastic scattering, and inelastic scattering. Elastic scattering

involves essentially no loss of the initial beam energy while inelastic scattering occurs with initial electron energy loss. Transitions within and out of energy states in an atom are generally caused by these inelastic collisions.

Even with the scattering and absorption of electrons, the electron beam can penetrate well into a solid. Measured in microns, the depth of penetration, d_p , of the electron beam at the spot onto which it is focused is given approximately by Equation 1. This depth is physically related to the acceleration of the electron beam and inversely to the density of the material. W_A is the atomic weight of an element A, V_o is the acceleration voltage of the electron beam, Z is the solid material's atomic number and ρ is the density of the solid material.

$$d_p = 11 \times 10^{-9} \frac{W_A \cdot V_o^2}{Z \cdot \rho} \quad (1)$$

There is one assumption that is implied here, the solid is composed of one element, A. For a solid with more than one element, the properties of the other elements must be factored in to accurately calculate the electron beam's interaction with the solid.

Looking back on Figure 2, radiation from the incident electron beam is uniformly distributed with respect to the beam. Little of the incident beam energy remains due to the overall efficiency of the process of absorption,

scattering, and heat generation. The energy loss, dE , of the incident electron beam is expressed in Equation 2.

$$dE = \rho \cdot f(E) \cdot dx \quad (2)$$

Here the solid has density ρ , and $f(E)$ represents an energy function that expresses the relative absorption coefficients of the solid in a penetration distance dx . Now use dn to express the number of atomic ionizations creating $K\alpha$ characteristic radiation from the incident electron beam on the solid. This ionization calculation is shown in Equation 3.

$$dn = C_A \cdot \rho_A \cdot \Psi_A(E, E_{K\alpha}) \cdot dx \quad (3)$$

C_A is the concentration of element A with density ρ_A . $\Psi_A(E, E_{K\alpha})$ is the $K\alpha$ ionization potential function for element A. The expression for ionization can be simplified as shown in Equation 4 by combining Equations 2 and 3.

$$dn = C_A \frac{\Psi(E, E_{K\alpha})}{f(E)} \quad (4)$$

In electron beam lithography, resolution, the dimension of the patterned feature, is driven by the size of the beam in the resist material. Scattering effects create the ionization processes needed to pattern the

resist, but they also effect resolution. The thickness of the film is a factor in the beam broadening effect. As the film thickness increases, the volume of material the electron beam interacts with increases. Beam broadening is a function of atomic number, film thickness, and acceleration voltage. This relationship is shown in Equation 5.

$$b = 625 \cdot \left(\frac{Z}{W \cdot V_0} \right) \cdot (\rho^{1/2} \cdot t^{3/2}) \quad (5)$$

W is the atomic weight, ρ is the density in g/cm^3 , V_0 is the acceleration voltage of the electron beam, and t is the film thickness in cm. Here, the Z and W terms are coefficients for each element in multielement materials. Beam broadening varies inversely with the acceleration voltage and increases with film thickness. An increase in acceleration voltage is needed for thicker films to compensate for the associated beam broadening.

Computer modeling can simulate trajectories of an electron in a solid to show the scattering paths for an electron beam. By modeling 10^3 to 10^4 trajectories, Monte Carlo statistics can simulate the electrons path in a solid. The output of such a model is shown in Figure 3. As the beam penetrates

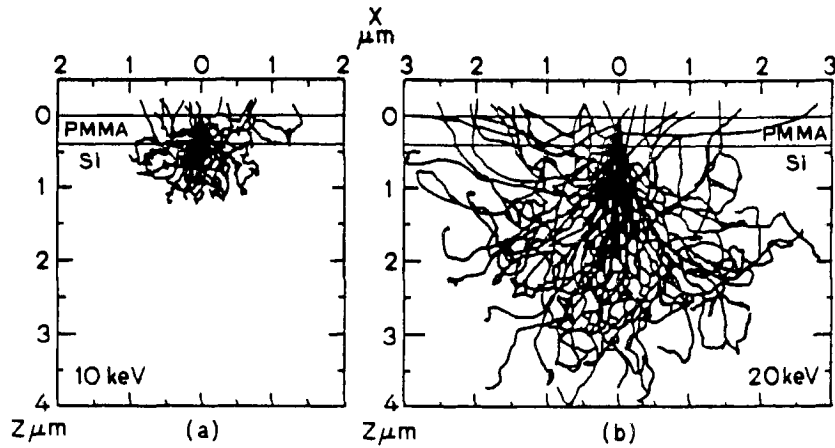


Figure 3. Simulated trajectories of electrons in a PMMA film on Si [7].

the resist layer, the effective width of the electron beam becomes larger than the beam's size upon entry. The direct effect of acceleration voltage is seen in this simulation. The electrons with the 10keV beam acceleration slow quickly and cause beam spreading without deeply penetrating the material. The 20keV beam has higher energy, and the electrons pass through the film with much less beam spreading. Not until they enter the underlying substrate, do the electrons scatter to significantly increase the beam width. The effective paths of the scattered initial and secondary electrons are one of the factors that determine the resist performance.

PMMA Radiation Chemistry

Electron beam resists are based on chemical and physical changes that effect the resist material. These changes are a result of exposure to a high energy electron beam, which enables the resist to be patterned. PMMA undergoes such changes when the ionizing radiation of the electron beam is directed into the PMMA film. The ionization process (Figure 4) of PMMA by high electron beam radiation is more efficient for inducing backbone chain scissioning compared to a deep UV photoexcitation processes.

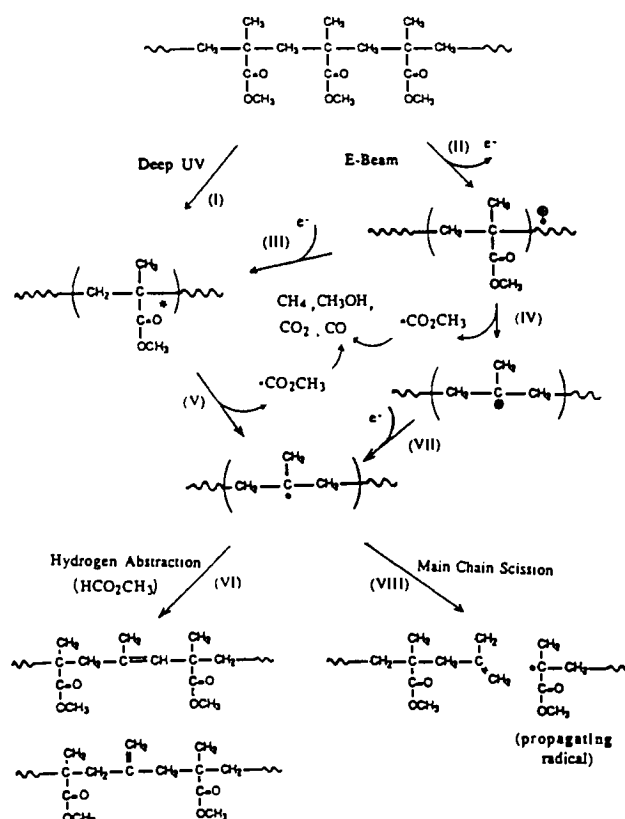


Figure 4. Schematic of decomposition paths for PMMA [8].

However, due to excess electrons in the sample during electron beam irradiation, cation radicals can be converted to excited state species similar to those produced by photoexcitation. This will decrease the amount of the main chain scissioning as hydrogen abstraction is more likely due to formation of methyl formate, HCO_2CH_3 . Without additional electron interaction, the cation radical will degrade to evolve a methyl formyl radical leaving behind a stable tertiary cation which is unlikely to undergo the abstraction process. The methyl formyl radical then decomposes to evolve gases such as CO , CO_2 , CH_4 , and CH_3OH . Here the gases are in greater quantities than the photoexcitation process, because in this case the methyl formyl radical does not abstract the hydrogen to form methyl formate. When the stable tertiary cation interacts with scattered or beam electrons and hydrogen abstraction does not occur, the polymeric backbone is broken as main chain scissioning occurs yielding a free radical [9]. This free radical can quickly propagate to efficiently fragment the polymeric backbone. However, this main chain scissioning can quickly stop as the double bond and the free radical are in close proximity and can recombine causing polymerization.

The PMMA resist is composed of PMMA resin and a casting solvent. Chlorobenzene has been the standard casting solvent used in PMMA resist applications. The solubility parameter of the casting solvent is a measure of how the PMMA resin dissolves into solution. Alternative solvents should have similar solubility parameters to chlorobenzene so performance

differences are minimized when comparing PMMA resist systems. The solvent behavior is an important factor for the pre-exposure bake where it is driven out of the film in order to improve adhesion, relax stress, and reduce pinholes. Solvent removal is important in minimizing any solvent-PMMA interactions during processing, such as increased solubility due to residual casting solvent. Table 1 lists the solubility parameters for the casting solvents used in this experiment. The solubility parameter is a measure of the cohesive energy density of a liquid solvent. The solubility parameters are used to match solvents against the solubility parameter of a polymer. This leads to predictions on the solubility of a polymer in a given solvent.

Solvent	Sol. Param.
PGMEA	9.6
Anisole	9.2
Butyl-acetate	8.5
Chlorobenzene	9.5

Table 1. Solubility parameters for experimental casting solvents [10,11].

Resolution and profile of the resist pattern depends on the electron beam energy distribution, amount of total exposure, and the solubility rate of the resist and developer systems. In PMMA resist, the exposed areas have greater solubility than the unexposed regions. Greater solubility is due to the scissioned fragments having lower molecular weight. Differential rates of dissolution is a major factor in image development. Solubility parameters of the developer solvent also control image development. The developer solvent must be chosen such that the dissolution of the unexposed regions

is low and the dissolution of the exposed regions is high [12]. The development process first uses a primary develop step then a secondary rinse step. The solvent used for the develop step must be a kinetically good solvent to penetrate into the film in order to begin the dissolution process. The second solvent used for the rinse step may have similar thermodynamic properties, but must be less of a kinetic solvent. Common developer solvents for PMMA resists are MIBK, methyl isobutyl ketone and IPA, isopropyl alcohol. To completely understand how solvents differ, the three principal forces of the solubility parameter must be compared. A solvent solubility parameter is composed of three principal forces, dispersive forces, permanent dipole forces, and hydrogen bonding forces. Table 2 lists these component parameters for the developer solvents MIBK and IPA. MIBK and IPA have similar thermodynamic characteristics with respect to PMMA. IPA alone does not act as a good developer. High hydrogen bonding forces prevent IPA from quickly penetrating deeply into PMMA. However, MIBK can quickly penetrate into PMMA to develop away the long organic backbone. Table 2 also lists these developer solvents in varying concentrations with their respective PMMA development performance parameters.

Developer	δ_d	δ_p	δ_h	Ro	(Å/min.)	β
IPA	7.75	3.0	8.6			
MIBK	7.49	3.0	2.8	84		3.14e8
1:1 MIBK:IPA	-	-	-	0		6.70e9
2:3 MIBK:IPA				0		9.37e12
1:3 MIBK:IPA			-	0		9.33e19

Table 2. Solubility principal force and develop parameters [13,14].

For the developer, R_0 is the removal rate for the unexposed regions of resist. Thickness loss of the unexposed regions upon development is directly attributed to this parameter. The β parameter is the coefficient for the removal rate of low molecular weight material. These development parameters are used in Equation 6, which describes the dissolution rate of the exposed resist [15].

$$R = R_0 + \beta \cdot M_f^{-\gamma} \quad (6)$$

Contrast of the resist is the γ parameter and is ideally as large as possible. Contrast is the measure of the change in solubility of the resist with increasing exposure. The value for contrast is calculated as the extrapolated slope of the remaining thickness versus exposure curve as the curve approaches the dose required to clear the resist thickness. Dose to clear, E_0 , is the minimum energy dose required to clear the original resist thickness.

The resist solubility is characterized by M_f , the fragmented molecular weight of the exposed resist. This fragmentation is dependent on the absorbed energy and the number of ionizations in the resist. M_f is calculated in Equation 7 using Avogadro's number, N_0 , the density of the resist material, ρ , and the number of ionizations, dn , from Equation 4.

$$M_f = \frac{dn}{\rho \cdot N_0} \quad (7)$$

Net ionization is lowered in PMMA due to the competing processes that occur in the degradation from ionization. This is seen as a higher sensitivity value for PMMA as an electron beam resist. Sensitivity is given as the dose required to achieve a solubility ratio of 50 for the exposed to unexposed regions of the resist. A general rule is that the sensitivity of the positive resist is independent of the initial molecular weight of the polymer [16]. However, that is not the case for resist systems with low net chain scissioning efficiency. Sensitivity is high due to the long exposure time required to change the solubility of the resist. Also, for an ideal resist, the initial dispersity should be low. Dispersity is a measure of the variation in the molecular weight of the polymer. With low initial dispersity, the chosen developer solvent will be less likely to dissolve portions of the high molecular weight, unexposed regions of the resist. This minimizes problems such as thickness loss, resolution degradation and image distortion when processing the resist.

EXPERIMENT

A three stage experiment was run to characterize the performance of variable molecular weight and alternative solvent PMMA resist systems. The first step was a screening experiment to determine coating thickness and solvent evaporation. Next, a designed experiment was used to find the optimal performance points for each specimen. Finally, confirmation runs were conducted at the optimal setpoints to verify output quality. The different resist configurations used for this experiment are listed in Table 3.

Sample Name	Manufacture Code	Solvent Used	Mw (g/Mol.)	Dispersity (Mw/Mn)	% Solids
CHLOR-1	C - 4 - 1	Chlorobenzene	577	3.3	4 %
CHLOR-2	C - 4 - 2	Chlorobenzene	614	5.4	4 %
CHLOR-3	C - 4 - 3	Chlorobenzene	539	4.0	4 %
CHLOR-4	C - 4 - 4	Chlorobenzene	589	3.3	4 %
CONTROL	C - 4 - C	Chlorobenzene	590	6.1	4 %
ANISOLE-4	A - 4	Anisole	589	3.3	4 %
ANISOLE-6	A - 6	Anisole	589	3.3	6 %
PGMEA-4	P - 4	(Propolyne glycol monomethyl ether	589	3.3	4 %
PGMEA-6	P - 6	acetate)	589	3.3	6 %
BUTYL-4	B - 4	Butyl-acetate	539	4.0	4 %
BUTYL-6	B - 6	Butyl-acetate	539	4.0	6 %

Table 3. PMMA resist systems used in experiment.

Screening Experiment

The screening experiment included three steps; wafer preparation, spin speed versus thickness determination, and manufactures' data on solvent evaporation. Four inch silicon wafers were used for substrates in this experiment. The wafers were cleaned using a two step ammonium

hydroxide and hydrochloric acid process. Table 4 lists the cleaning process used during the experiment.

NH ₄ OH/H ₂ O ₂ /H ₂ O in a 1:1:5 ratio @ 75-80°C for 10 minutes
DI water rinse for 5 minutes
HF/ H ₂ O in a 1:10 ratio for 1 minute
DI water rinse for 5 minutes
HCL/H ₂ O ₂ /H ₂ O in a 1:1:5 ratio @ 75-80°C for 10 minutes
DI water rinse for 10 minutes
Spin dry wafers
Bake wafers @ 100°C for 60 minutes

Table 4. Steps for wafer cleaning process.

After the clean and bake process, the wafers were cooled to room temperature for spin coat application of the experimental resists. A Convac 601 reticle-plate spinner with a chuck modified to hold four inch silicon wafers was used for the spin coating process. The spinner was controlled manually, and calibrated for spin speeds with a hand held tunable strobe. The resist was dispensed from a pipet onto the stationary wafer. The wafer was immediately accelerated with maximum ramp rate to the desired spin speed and held for 45 seconds. Each wafer was then pre-(exposure)baked on the vacuum hot-plate for two minutes at 165°C. All of the samples were coated in this manner [17]. After the coating and pre-bake process, each wafer was measured with a Nanospec IV spectrophotometric thickness measurement tool to obtain resist thickness. The spin coat, pre-bake and measurement process was repeated at varying spin speeds to capture a 4000Å target resist thickness for each sample.

The evaporation characteristics of the solvents in each resist system were used to determine the operational range for the resist pre-bake. The solvent evaporation data was gathered and provided by the manufacturer, Microlithography Chemical Corporation of Watertown, MA. Chlorobenzene, butyl-acetate, anisole, and PGMEA were cast in 4% solids resist solutions. The solutions were baked on a laboratory hot plate from 150°C to 200°C. Weight percent of solution remaining was measured at 30 second intervals up to five minutes. Temperature was adjusted until all samples had evaporation rates similar to the control solvent, chlorobenzene. The manufactures' detailed conditions and results of this study are found in Appendix B.

Optimization Experiment

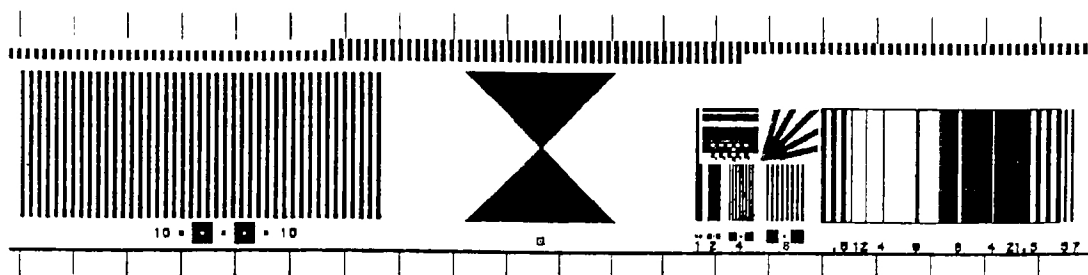
A three-factor central-composite response surface design was used to find the optimal operating range for each resist sample. Input factors investigated were pre-bake temperature, exposure dose, and development time. These factors were selected due to their known effects on resolution, contrast, and thickness loss. Table 5 lists the experimental conditions for each sample in this experiment.

Sample	Pre-Bake (°C)	Exposure ($\mu\text{C}/\text{cm}^2$)	Development (sec.)
Control	160,170,180	0 120, by $5\mu\text{C}$ steps	30, 45, 60
Chlor-1	160,170,180	0 - 120, by 5	30, 45, 60
Chlor-2	160,170,180	0 120, by 5	30, 45, 60
Chlor-3	160,170,180	0 - 120, by 5	30, 45, 60
Chlor-4	160,170,180	0 120, by 5	30, 45, 60
Anisole-6	175,185,195	0 - 120, by 5	30, 45, 60
PGMEA-6	175,185,195	0 120, by 5	30, 45, 60

Table 5. Conditions for experimental optimization.

Four samples, Butyl-6, Butyl-4, Anisole-4, and PGMEA-4 could not be spin coated to the required thickness. For this reason, they were not included in the optimization experiment while the remaining seven samples were tested. Three output responses were measured for each resist sample, these were: dose to clear, E_0 ($\mu\text{C}/\text{cm}^2$); contrast, γ ; and thickness loss, T_0 (\AA).

Separate experiments were run in random order for each of the seven samples. Within each experiment, ten wafers were run in random order at the experimental conditions. The same procedure was followed for each wafer, within each experiment. The wafers were spin coated with the sample resist and pre-baked at the specified experimental temperature. The resist coated wafer was then placed in a MEBES-I electron beam writing system for resist exposure. The resist was exposed to the resolution test pattern shown in Figure 5.



The measured responses were analyzed using RS/1 and JMP statistical software. Contour plots were constructed for contrast and dose to clear for ranges of develop time and pre-bake temperatures; listed in Appendix E for reference. Optimal points for these two factors were found to maximize contrast while minimizing dose to clear at input values within the experimental range. At the optimal develop time and pre-bake temperature, additional wafers were run for each sample to gather pattern dimension data. Linewidth measurements were obtained from the 4 μ m lines in the resolution test pattern using a Nikon 2I laser measurement system. Plots were made using the measured line data at varying exposures; listed in Appendix F. As the curve asymptotically approaches the target dimension, an optimal exposure dose is chosen. The exposure selected is at a point where variations in exposure should not significantly alter the linewidth. These pre-bake temperature, exposure dose, and develop time values were used to determine the optimal operating conditions for each resist sample.

Confirmation Runs

Confirmation runs for each resist sample were carried out at the calculated optimal setpoints. Fifteen constant exposure sites of the test pattern were written across each wafer. Thickness measurements were taken to determine resist coating uniformity. A randomly selected 10 μ m line was measured 10 times at each of the 15 patterns. This linewidth data was used to quantify resist performance across the wafer.

RESULTS AND DISCUSSION

Screening Experiment

Eleven samples were studied, seven of which were found suitable for processing. The target resist thickness was 4000\AA ($\pm 200\text{\AA}$) for this experiment. Figure 6 plots the response curve for thickness at various spin speeds for ten of the samples studied.

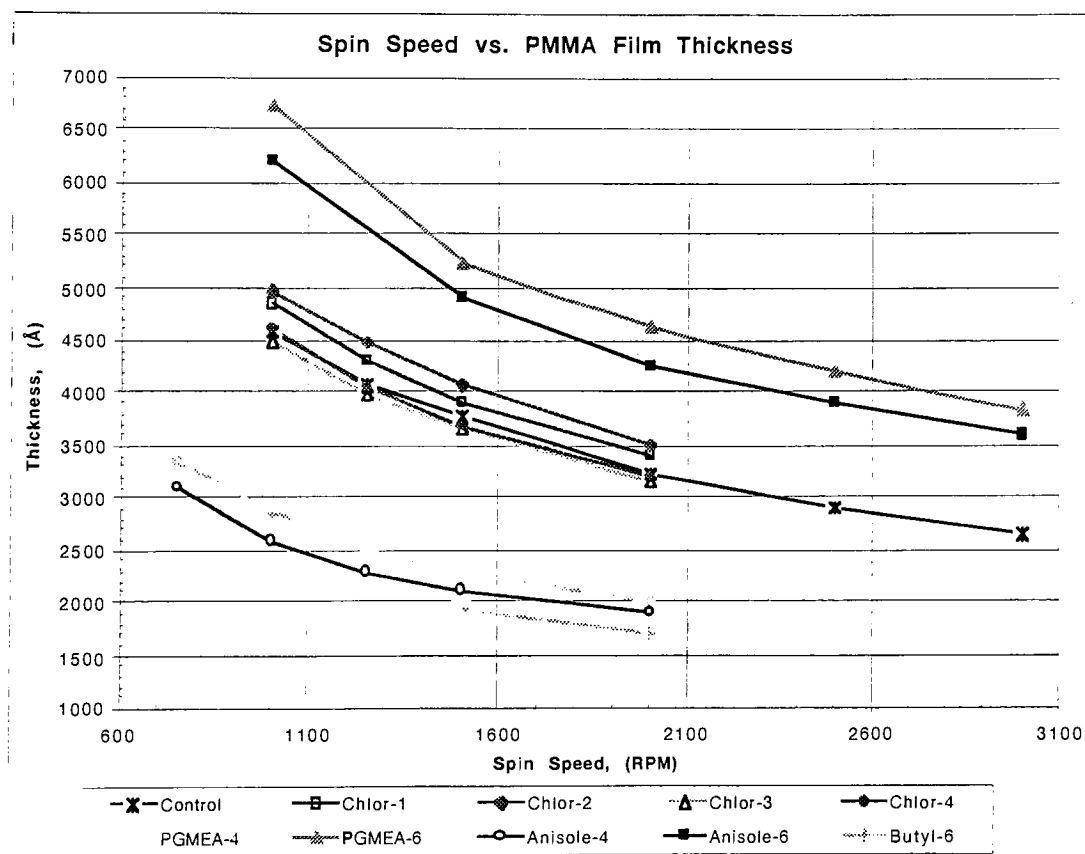


Figure 6. Spin speed coating characteristic curves of samples studied.

Samples, Butyl-4, Butyl-6, Anisole-4, and PGMEA-4 could not be cast to the desired thickness within a desirable spin speed range. The solubility parameters for the alternative solvents show a practical difference when put into practice as Butyl-Acetate is too thin while Anisole and PGMEA require higher solid contents. Spin speeds of much less than 1000 RPM would be required for the four samples to cast near 4000Å. At spin speeds much less than 1000 RPM, the resist can suffer from poor coating uniformity, adversely affecting lithographic performance. The remaining seven samples, Control, Chlor-1, Chlor-2, Chlor-3, Chlor-4, Anisole-6, and PGMEA-6 were cast to the 4000Å thickness target within the 1200 to 2800 RPM range. Table 6 lists the calculated spin speed to obtain the experimental target resist thickness. The actual thickness listed for each sample in table #6 is the measured thickness during the experiment.

Sample	Spin Speed (RPM)	Thickness (Å)
Control	1325	4027
Chlor-1	1450	4066
Chlor-2	1575	4058
Chlor-3	1250	4107
Chlor-4	1300	4011
Anisole-6	2400	4033
PGMEA-6	2800	4011

Table 6. Calculated spin speeds for experimental samples.

The evaporation characteristics varied significantly between the experimental solvents. The baseline solvent for comparison is

chlorobenzene, which has generally been the standard casting solvent for PMMA resist systems. The evaporation rate baseline for comparison is a moderate evaporation rate, where approximately 30% solvents by weight remain after a two minute bake. The fast and slow evaporation rates vary by up to one minute around the moderate range. The tabulated summary of evaporation rates is listed in Table 7. The letters C, P, A, and BA correspond to chlorobenzene, PGMEA, anisole, and butyl-acetate respectively. The numbers 150 to 200 are temperatures in °C.

Samples	Evap. Rate % at 2min.	
A-150, P-150	Slow	50 %
C-150, A-175, A-185, A-200, P-175, P-185, P-200, BA-150	Moderate	30 %
BA-175, C-185, C-175, BA-185	Fast	10 %

Table 7. Grouped sample evaporation rates.

Here the butyl-acetate solvent behaves similar to the chlorobenzene at each temperature tested. From 150°C to 185°C, these two solvents tracked from moderate to fast evaporation rates. The anisole and PGMEA solvents gave much slower evaporation rates than chlorobenzene or butyl-acetate at similar temperatures. The anisole and PGMEA solvents performed in the moderate evaporation range when temperatures were elevated 20 to 30°C. With higher evaporation rates to achieve similar solvent content, the anisole and PGMEA resists need to be pre-baked at 20 to 30°C higher temperatures. This difference in pre-bake temperature is seen in the

experimental setup, Table 5. The chlorobenzene resists were pre-baked with 160 to 180°C ranges, while the anisole and PGMEA resists were pre-baked with 175 to 195°C ranges. Figure 7 illustrates the different bands of evaporation rates for the experimental solvents. These rate groups are seen as gentle slopes for the slow solvents, and steeper slopes for the faster solvents.

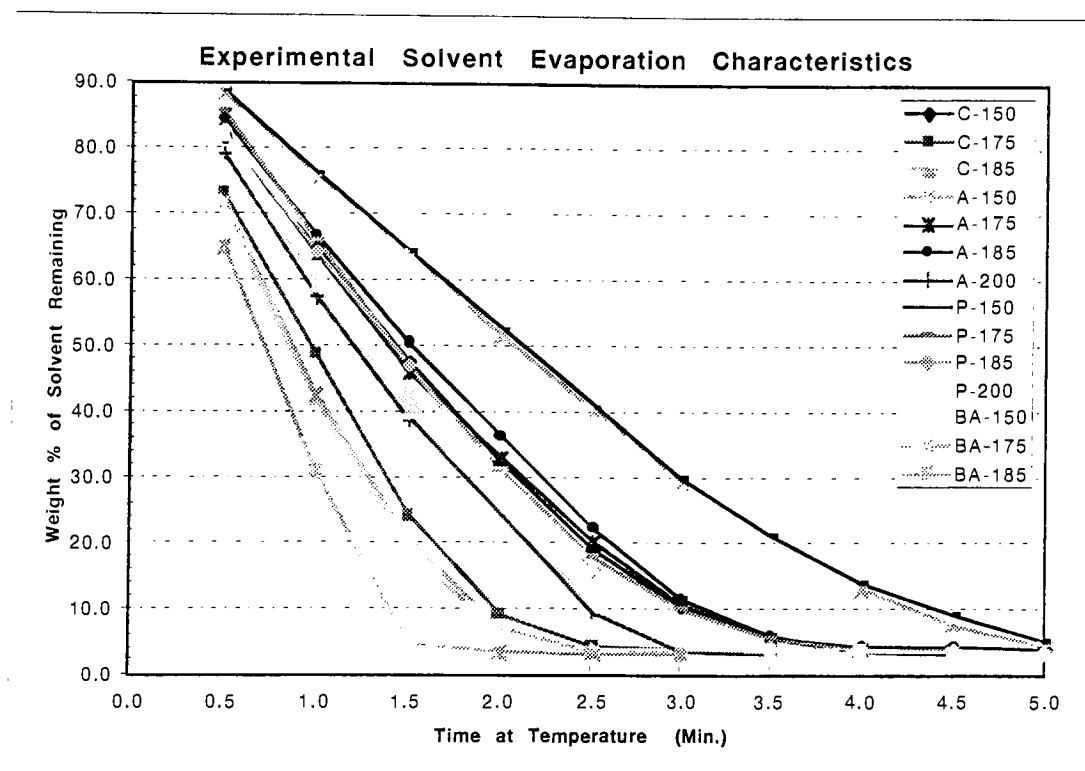


Figure 7. Evaporation rate for experimental solvents.

Optimization Experiment

Contrast did not significantly vary between the different experimental samples. For each M_w and solvent sampled, differences in contrast could not be distinguished by a statistical T-test. The T-test evaluates distributions for a statistically significant difference between them. The T-tests in Figure 8 show that contrast does not vary significantly for the different experimental solvents or M_w 's. Additional T-tests indicated contrasts were comparable across experimental resist samples and molecular weight dispersities.

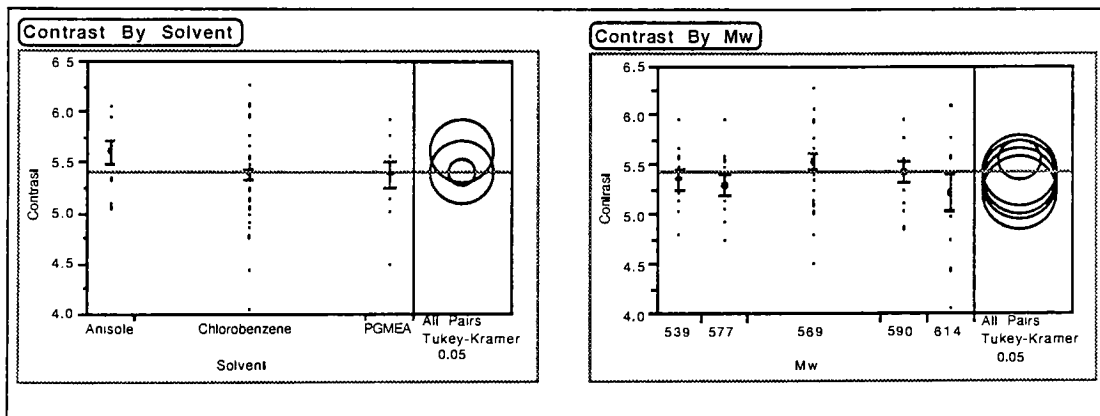


Figure 8. T-tests of contrast for each experimental solvent & M_w .

Contrast was primarily controlled by develop time. Higher develop times reduced the contrast performance of each resist. Develop time also controlled E_0 , dose to clear. However, pre-bake temperature also affected dose to clear. This is an interaction, where two factors simultaneously

control an output response. This interaction is illustrated in Figure 9 as a summary of experimental contrast curves. The complete set of experimental contrast curves and the measured thickness data can be referenced in Appendix D.

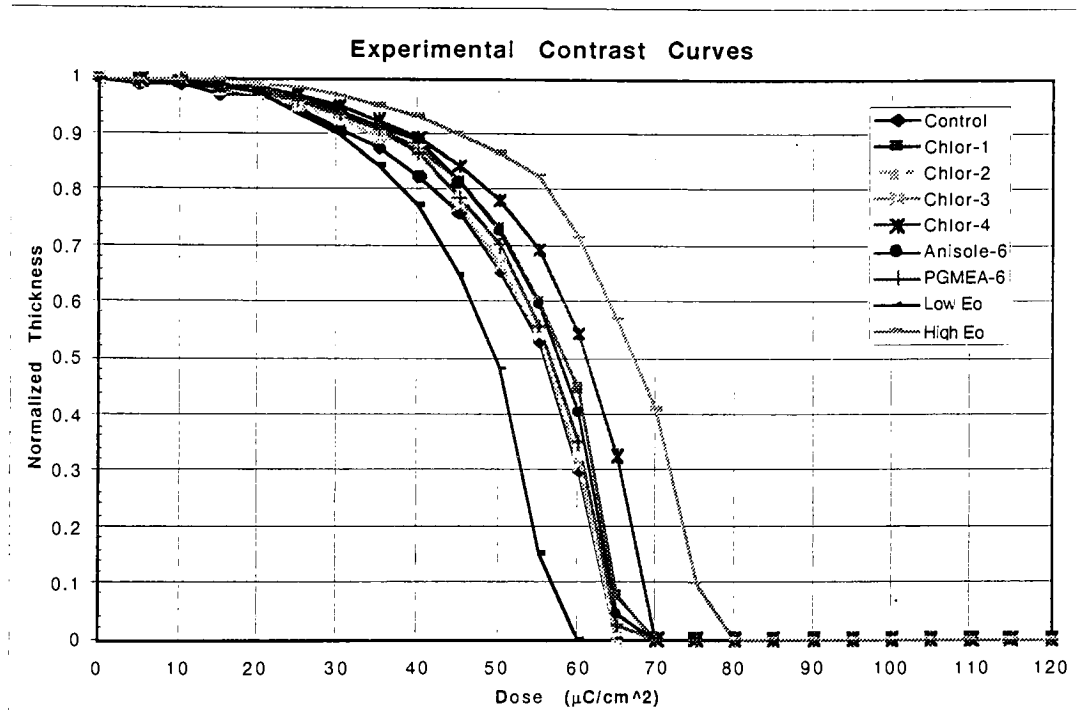


Figure 9. Midpoint contrast curves, bordered by high & low E_0 , curves.

The low E_0 contrast curve in Figure 9 corresponds to a low pre-bake temperature and the longest develop time. On the other side, higher E_0 contrast curves result from higher pre-bake temperatures and shorter develop times. The remaining contrast curves are for experimental cell with midpoint parameters. Like contrast, dose to clear did not vary for any

particular experimental resist sample. This is illustrated with the T-test comparison in Figure 10. Solvent type, M_w , or dispersity also had no singular affect.

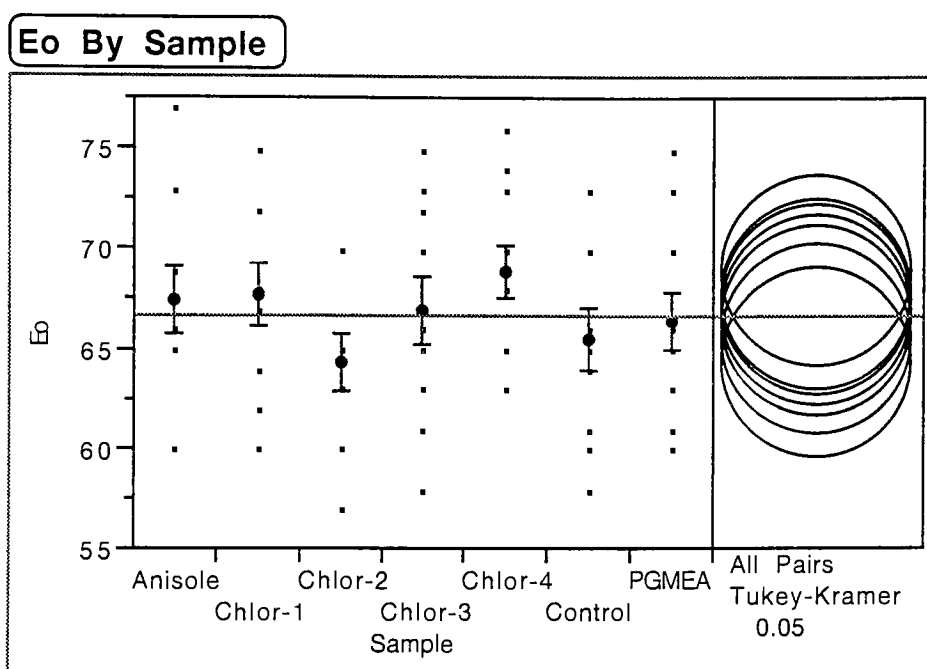


Figure 10. T-test of Dose to Clear (E_0) for each experimental sample.

Thickness loss, T_0 , at zero exposure quantifies the effect of developer solvent on a resist system. Thickness loss was not well modeled in this experiment. Average thickness loss was slightly higher at lower develop times. This opposite of what was expected. However, looking at the raw data, sample Chlor-3 is seen to have significant variation in T_0 . With the Chlor-3 outlier data removed, the thickness loss is seen to be less than 5\AA for the remaining samples. This is expected as the 1:1, MIBK:IPA solvent

developer has a low rate of dissolution for unexposed, high M_w resist material.

Output analysis of the designed experiment confirms the effects observed analyzing the contrast curves. Figure 11 shows the relationship between the measured responses and the experimental input factors.

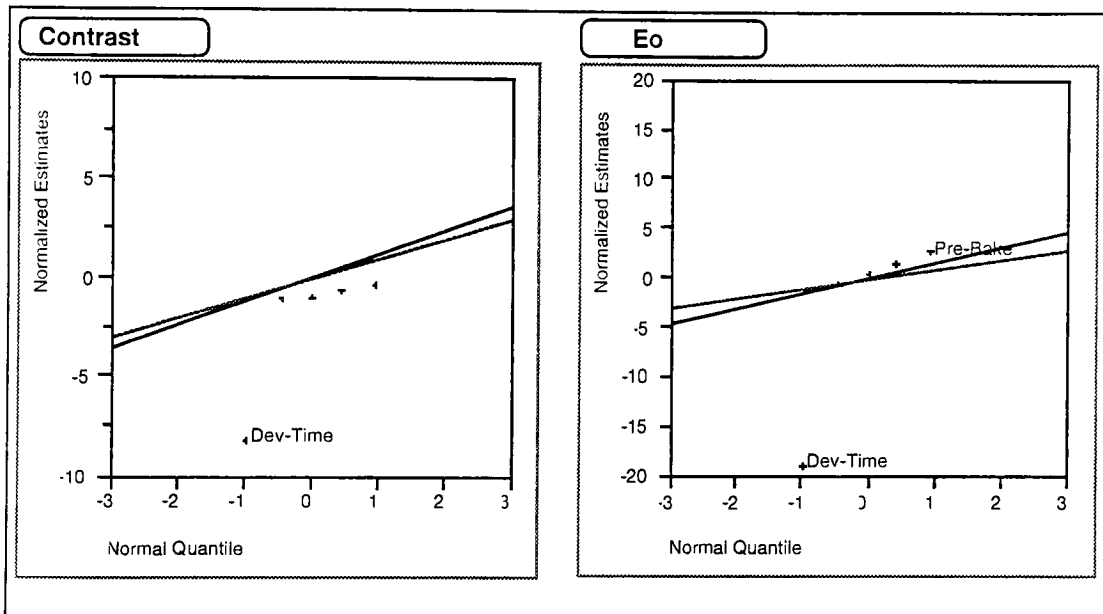


Figure 11. Normal probability plots for responses contrast and E_0 .

From the normal probability plots of experimental factors, develop time is identified as statistically significant main factor for both responses. Pre-bake temperature has a significant affect only on E_0 . The impact of the factors on each response can be seen in an effect plot. The effect plots in Figure 12 show the significance of the pre-bake temperature and develop time factors on contrast and E_0 . When develop time increases, contrast and E_0 decrease.

As pre-bake temperature increases, E_0 increases. While pre-bake temperature has a statistically insignificant effect on contrast, its effect on contrast can be seen at higher temperatures.

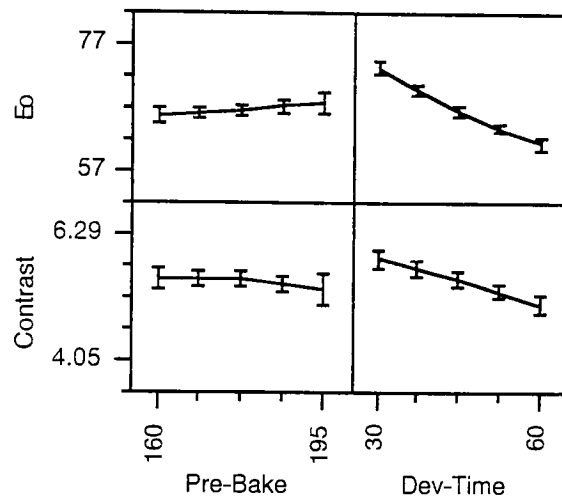


Figure 12. Effect plots of responses to input factors.

From the effect plots, increasing develop time degrades contrast while improving dose to clear. An optimal develop time cannot be determined by moving only develop time within the experimental window. Pre-bake temperature also effects the output responses. The response to this effect needs to be combined with the response to develop time. A contour plot determines the effect of two input factors on a single response. Figure 13 has two overlay contour plots of contrast and E_0 for this experiment, based on two input parameters solvent and M_w . The individual contour plots and analysis of variance for each sample resist are referenced in Appendix E.

With each overlay contour plot, contrast can be maximized while keeping a minimal dose to clear. Utilizing the contour plots of each sample resist, pre-bake temperature and develop time were selected to maximize contrast.

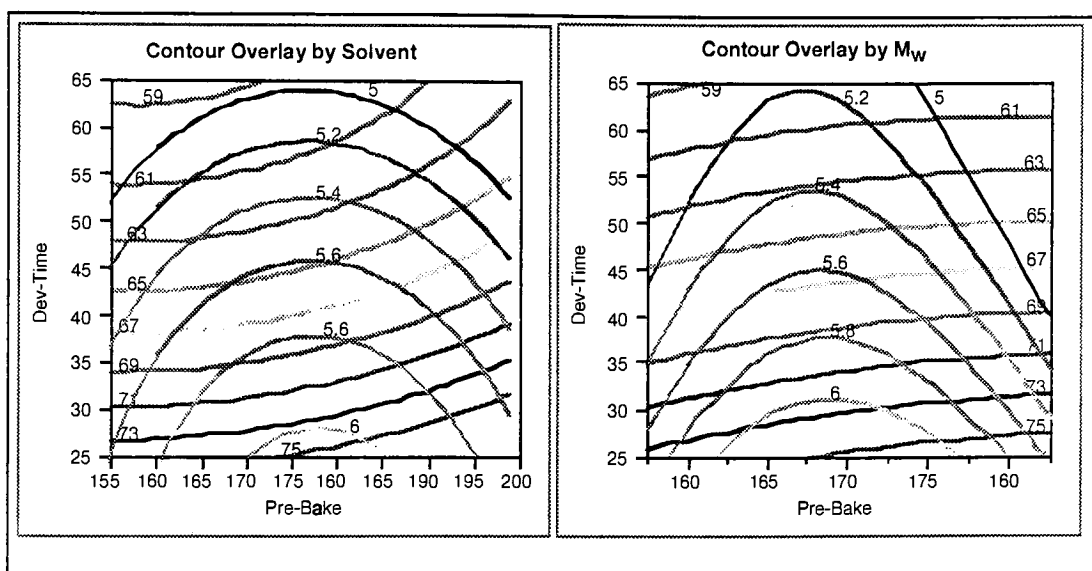


Figure 13. Summary contour plots for responses contrast and E_0 .

The optimal develop time and pre-bake temperature selected from the contour plot of each resist type are summarized in Table 8.

Sample	Pre-bake (°C)	Dev. time (s)
Chlor-1	171	42
Chlor-2	168	50
Chlor-3	166	45
Chlor-4	167	40
Control	170	45
Anisole-6	182	45
PGMEA-6	182	45

Table 8. Optimal input factors calculated from contour plots.

As expected, pre-bake temperature only varies significantly by the casting solvent. While develop time only varied by 3 to 5 seconds around the mean, it did follow a more subtle resist parameter. Initial molecular weight dispersity was seen to have a small but insignificant effect on the resist system performance. Develop time increased with increasing dispersity of PMMA resin. As a greater range of molecular weights are needed to be dissolved, the develop time must be extended to prevent the higher molecular weight material from remaining in the exposed areas. However, develop time did not significantly increase with increasing molecular weight.

The needed exposure dose was determined by measuring linewidth dimensions at the optimal develop time and pre-bake temperature. The linewidth versus exposure curve in Figure 14 illustrates the effect of exposure dose on linewidth dimension. Linewidth curves for all samples are located in Appendix F for reference.

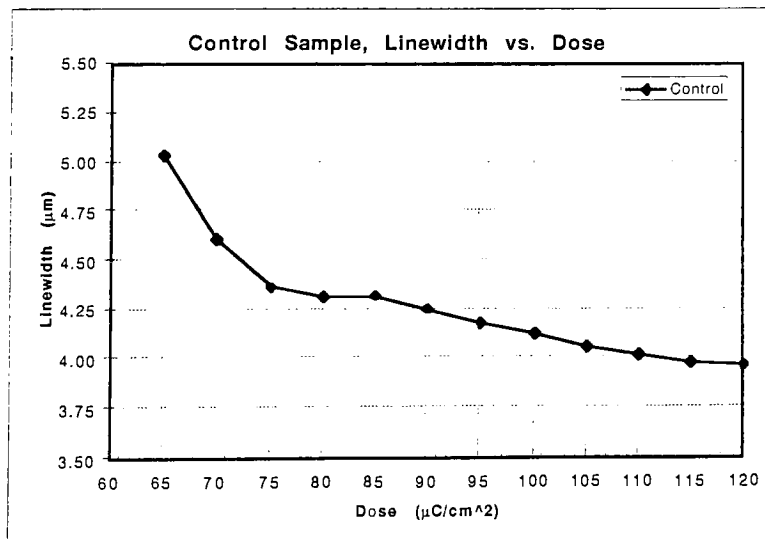


Figure 14. Plot of measured linewidth versus exposure dose.

The exposure dose used for patterning each resist sample is calculated from the linewidth plot. The desired dose is selected where changes in exposure have a minimal effect on the measured linewidth. An 80 $\mu\text{C}/\text{cm}^2$ target has a process tolerance of 5 μC for the control sample as seen in Figure 14. The exposure dose for each resist is listed in Table 9.

Sample	Pre-bake ($^{\circ}\text{C}$)	Dev. time (s)	Dose ($\mu\text{C}/\text{cm}^2$)
Chlor-1	171	42	95
Chlor-2	168	50	85
Chlor-3	166	45	90
Chlor-4	167	40	95
Control	170	45	80
Anisole-6	182	45	90
PGMEA-6	182	45	85

Table 9. Optimal input factors calculated from experimental analysis.

Confirmation Runs

Confirmation runs using the optimal processing factors from Table 9 showed no statistically significant difference between the samples. The effects of dispersity, M_w and exposure on linewidth are shown in Figure 15.

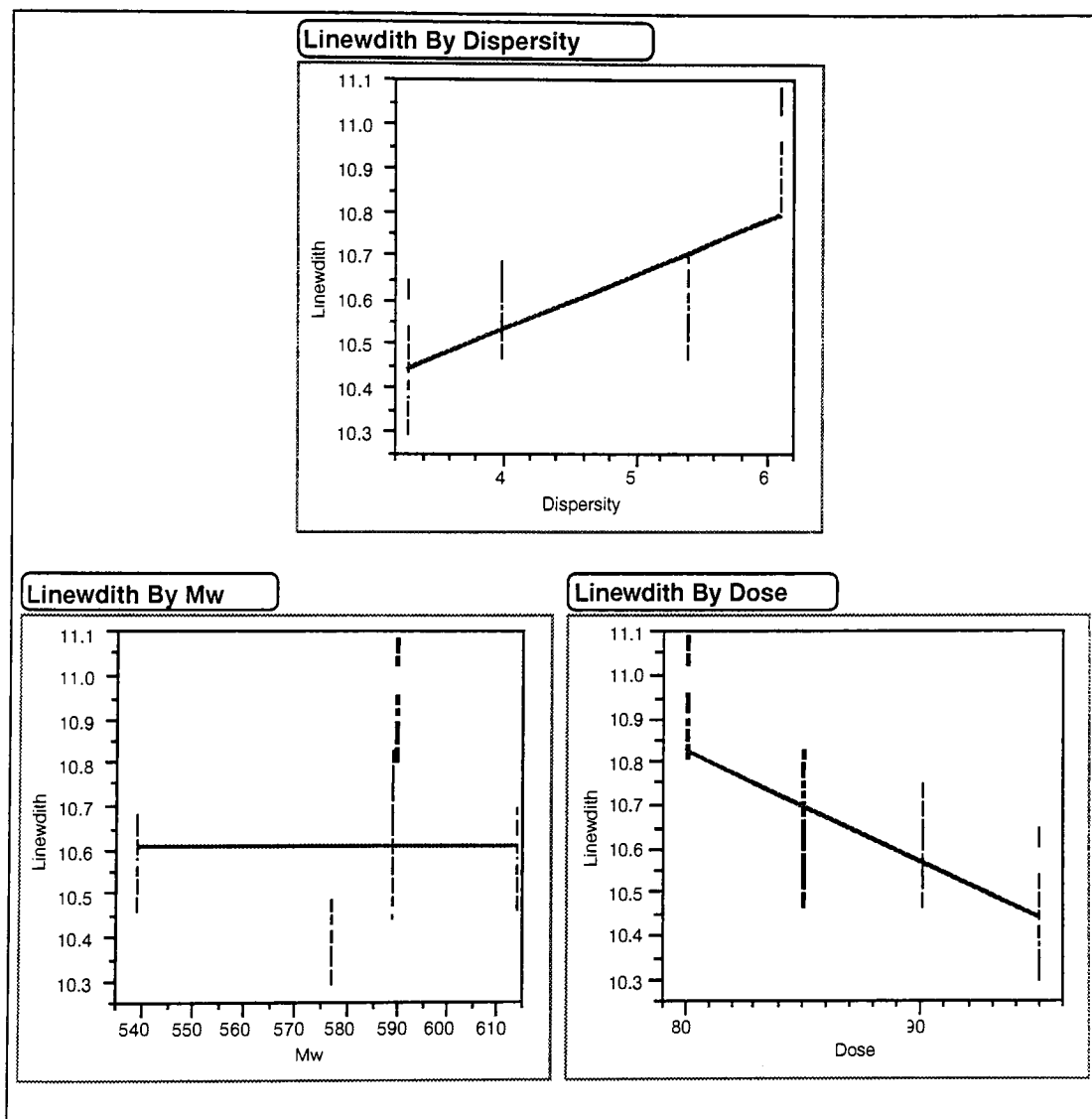


Figure 15. Effect of dispersity, M_w and dose on linewidth.

Analysis of the linewidth data showed that M_w had no significant effect on resist performance. However, linewidth decreases with increasing exposure. This was seen in Figure 14 where the exposure dose for patterning was selected. As dose increases, the polymer chains in the exposed regions become more fragmented. This leads to better dissolution of the exposed regions by the developer, and subsequently smaller linewidths. Analysis of the dispersity data shows that there is a trend of higher dispersity material causing larger deviations from the targeted linewidth.

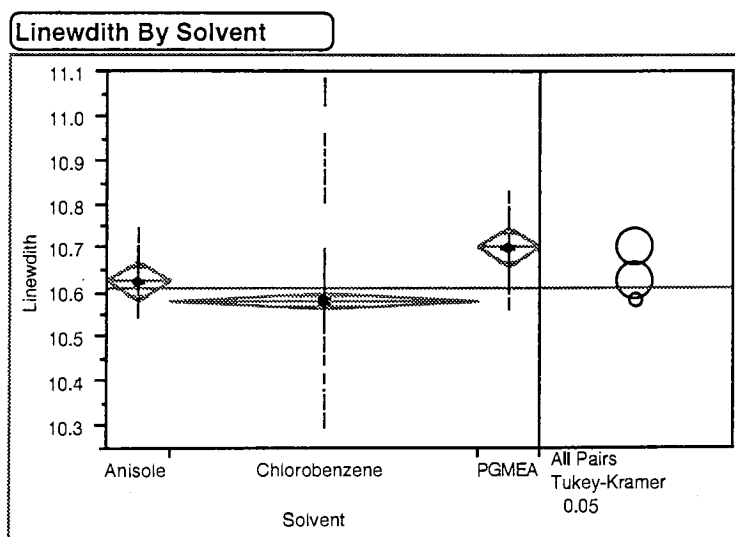


Figure 16. T-test of linewidth for each experimental solvent.

Solvent did not have a statistically significant effect on the linewidth output. The T-test in Figure 16 illustrates the overlapping ranges of linewidth for each experimental solvent. The linewidth data is referenced in Appendix G.

CONCLUSIONS

The PMMA samples evaluated, resulted in equivalent performance given similar process input factors. Measured output responses did not vary with statistical significance. Variation in measured linewidth output was minimal (1.6% 1σ) during the confirmation runs. Optimal process input parameters (Table 10), pre-bake temperature, develop time and exposure dose, did not have to be significantly altered to achieve similar outputs.

Sample	Optimal Inputs			Experimental Results		
	Pre-bake (°C)	Dev. time (s)	Dose ($\mu\text{C}/\text{cm}^2$)	Contrast	Dose to Clear	Thickness Loss
Chlor-1	171	42	95	5.3	68	8
Chlor-2	168	50	85	5.2	64	6
Chlor-3	166	45	90	5.4	67	9
Chlor-4	167	40	95	5.6	69	2
Control	170	45	80	5.4	66	6
Anisole-6	182	45	90	5.6	68	1
PGMEA-6	182	45	85	5.4	66	2

Table 10. Optimal input factors with summary experimental results.

Table 10 lists the samples that received complete experimental optimization. Four of the eleven original samples were shown not capable. Butyl-Acetate did not match well to PMMA as a casting solvent. The solubility parameter, while similar to PMMA, did not work in practice. Anisole-4 and PGMEA-4 could not be cast as a suitable resist film. Higher percent solids solutions (6%) were used to test these two solvents.

Pre-bake temperature was the only parameter dependent on the casting solvent. Anisole and PGMEA needed to be pre-baked at a 10 to 15°C higher temperatures than chlorobenzene. This parameter can be easily set and will not effect the application and processing of these solvents in PMMA resists. Anisole and propylene glycol monoethyl ether acetate perform with statistical and practical equivalence to chlorobenzene based PMMA resist systems. Anisole and PGMEA are two suitable safe solvent candidates for replacing chlorobenzene.

The M_w of the experimental samples showed no statistically significant effect on the measured responses. However, while not statistically significant, the molecular weight dispersity did have an effect. Low dispersity material is needed to prevent patterned linewidth deviations. The molecular weight range from 539,000 g/mol to 614,000 g/mol evaluated showed no significant effects in processing PMMA resist. Commercially supplied PMMA resin held within this range provides acceptable results.

The samples evaluated provided acceptable results as replacements for chlorobenzene based PMMA resists with the range of PMMA molecular weight supplied. Two items for future work are recommended to understand at what point processing outputs may be affected. A wider range of molecular weights can be evaluated to determine when incoming M_w variation causes processing problems. Also, testing can be done to better quantify the effect of dispersity on processing performance.

REFERENCES

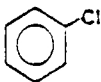
1. R.C. Tiberio, J.M. Limber, G.J. Galvin, and E.D. Wolf, "Electron Beam Lithography and Resist Processing for the Fabrication of T-Gate Structures," SPIE, vol. 1089, p. 124, 1989.
2. K. G. Chiong, M.B. Rothwell, S. Wind, J. Bucchignano, "Resist Contrast Enhancement in High Resolution Electron Beam Lithography," J. Vac. Sci. Technol. B, vol. 7, no. 6, p. 1771, Nov/Dev 1989.
3. N. Samoto, Y. Makino, K. Onda, E. Mizuki, and T. Itoh, "A Novel Electron Beam Exposure Technique for 0.1 μm T-Shaped Gate Fabrication," J. Vac. Sci. Technol. B, vol. 8, no. 6, p. 1335, Nov/Dev 1990.
4. C.P. Wong, "Polymers for Electronic and Photonic Applications," Academic Press, San Diego, CA 1993.
5. P. Zant, "Microship Fabrication: A Practical Guide to Semiconductor Processing," McGraw Hill, NY 1990.
6. L.E. Murr, "Electron and Ion Microscopy and Microanalysis," Marcel Dekker, Inc., NY 1982.
7. D.F. Kyser, N.S. Viswanathan, "Monte Carlo Simulation of Spatially Distributed Beams in Electron-Beam Lithography," J. Vac. Sci. Technol., vol. 12, no. 6, p. 1335, Nov/Dev 1975.
8. J.O. Choi, J.A. Moore, J.C. Corelli, J.P. Silverman, H. Bakhru, "Degradation of Poly(methylmetacrylate) by Deep Ultraviolet, X-Ray, Electron Beam, and Proton Beam Irradiations," J. Vac. Sci. Technol. B, vol. 6, no. 6, p. 2286, Nov/Dev 1988.

9. A. Reiser, "Photoreactive Polymers (The Science and Technology of Resists)," Wiley Interscience, NY, 1989.
10. F. Rodriguez, "Principles of Polymer Systems," McGraw Hill, NY 1985.
11. R.B. Seymour, C.E. Carraher, "Polymer Chemistry; An Introduction," Marcel Dekker, Inc., NY, 1988.
12. P.A. Lamarre, "Developer Selection for T-Shaped Gate FET's Using PMMA/P[MMA-co-MAA]/PMMA," IEEE Trans. Electron Devices, vol. 39, no. 8, p. 1844, Aug. 1992.
13. S. Wolf, R.N. Tauber, "Silicon Processing for the VLSI Era," Lattice Press, Sunset Beach, CA 1986.
14. C. Hansen, "The Three Dimensional Solubility Parameter," Journal of Paint Technology, vol. 39. No. 505, p. 104, Feb. 1967.
15. J.S. Greeneich, "Developer Characteristics of Poly-(Methyl Methacrylate) Electron Resist," J. Electrochem.: Solid-State Sci. Technol., vol. 122, no. 7, p. 970, Jul. 1975.
16. J.A. Delaire, M. Lagarde, D. Broussoux, and J.C. Dubois, "Effects of molecular weights and polydispersity on the properties of poly(trifluoroethyl methacrylate) as a positive x ray and electron resist," J. Vac. Sci. Technol. B, vol. 8, no. 1, p. 33, Jan/Feb 1990.
17. D.E. Bornside, C.W. Macosko, and L.E. Scriven, "Spin Coating of a PMMA/Chlorobenzene Solution," J. Electrochem. Soc., vol. 138, no. 1, p. 317 Jan. 1991.

APPENDIX A

Chlorobenzene Material Safety Data Sheet

Appendix A (Cont.)

IDENTIFICATION	NTP PREFERRED NAME: Chlorobenzene Synonyms: Monochlorobenzene Phenylchloride	
	CAS Registry Number: 108-90-7	
	NIOSH Registry Number: 000175J00	
	Formula: C ₆ H ₅ Cl Molecular Weight: 112.56 MLN: GR	
PHYSICAL DATA	Physical Description: Colorless, very refractive liquid.	
	Melting Point: -45°C	Boiling Point: 131-132°C
	Density: 1.1053 g/mL	Specific Gravity: 1.11 at 20°/20°C
	Flammability: Flammable	Stability: Sensitive to heat and oxidizers.
	Flash Point: 29°C (84°F)	
	Reactivity: Reacts violently with AgClO ₄ and other strong oxidizers, dimethyl sulfoxide, heat and/or flame.	
	Solubility In:	
	Water: 0.3 /100 g at 20°C	Acetone: Not available
	DMSO: Not available	Ether: Very soluble
	Ethanol: Very soluble	Benzene: Very soluble
Other Physical Data: Very soluble in chloroform, carbon tetrachloride and carbon disulfide. Almond-like odor. Explosive Limits: 1.3% Lower, 7.1% Upper. Vapor pressure is 3.3 mm Hg at 20°C; vapor density is 3.9.		
REGULATIONS	D.O.T. Shipping Name: Chlorobenzene (RQ-100/45.4)	
	D.O.T. Identification Number: UN1134	
	D.O.T. Hazard Classification: Flammable liquid	
	Other Shipping Regulations: Flammable liquid label required. Passenger limit is 1 quart; cargo limit is 10 gallons.	
	Exceptions: 173.118. Specific requirements. 173.119 in Hazardous Materials Regulations of the Department of Transportation (1981).	

Appendix A (Cont.)

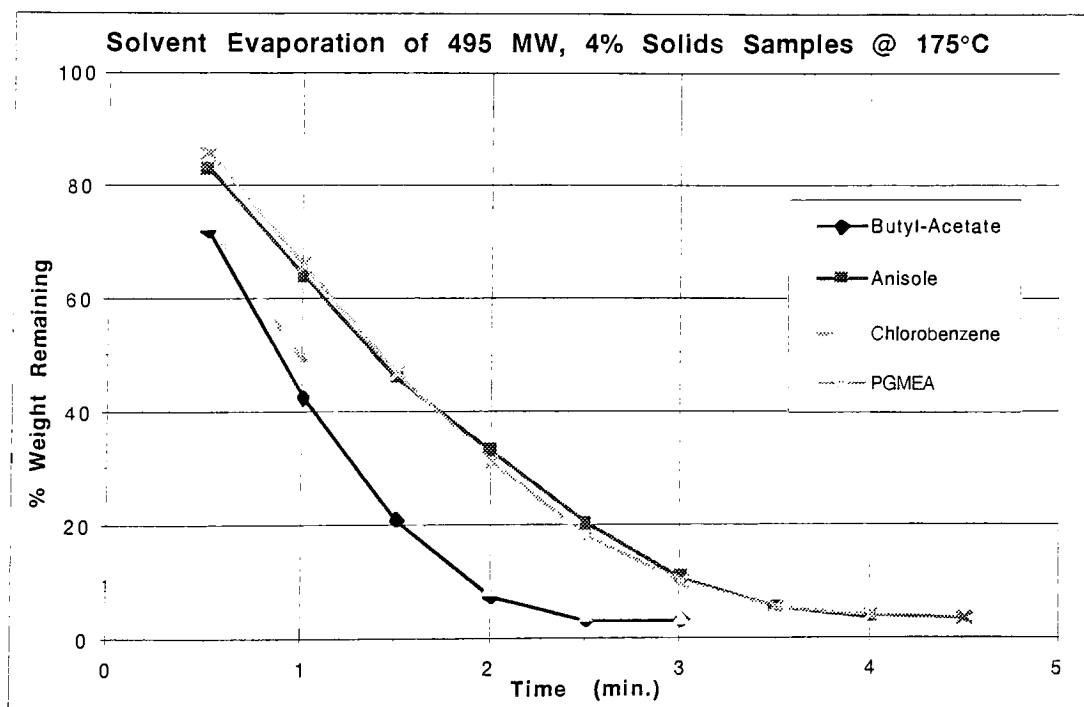
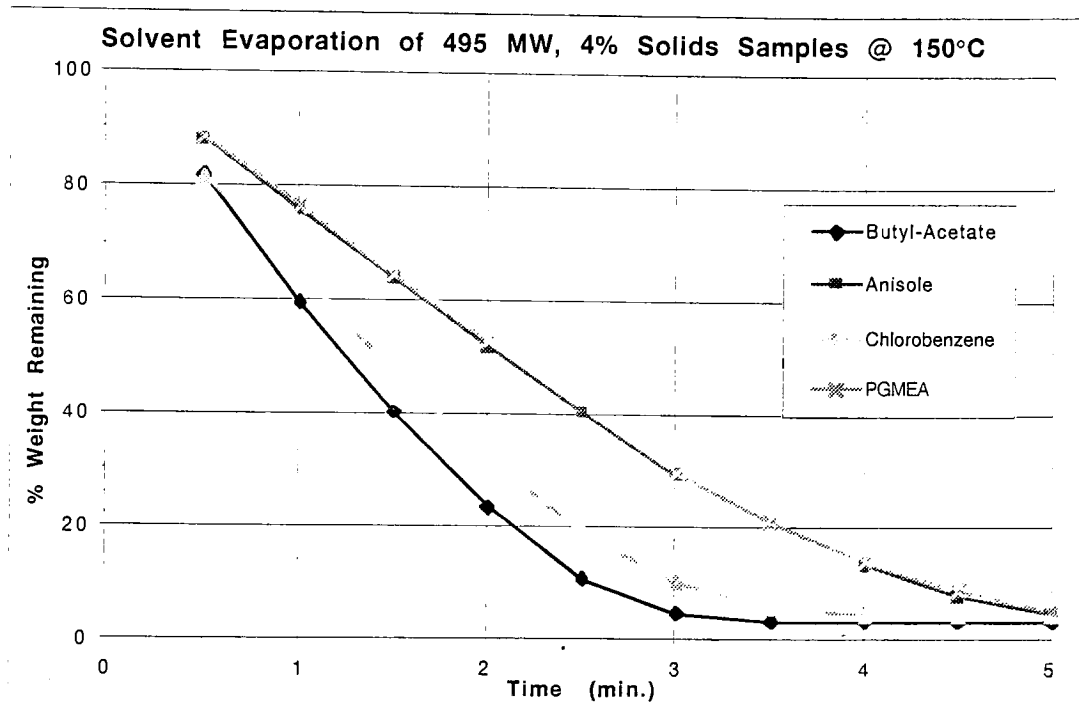
NTP PREFERRED NAME: Chlorobenzene

<p>Acute Hazards: Toxic, narcotic effects, irritant, hazardous decomposition products.</p> <p>Symptoms: Somnolence, loss of consciousness, twitching of extremities, cyanosis, rapid respiration and weak, irregular pulse. Irritation to eyes, nose and throat.</p> <p>Exposure Limits: ACGIH has adopted a TLV-TWA of 75 ppm (350 mg/m³). NIOSH-OSHA gives permissible exposure limit of 75 ppm and concentrations of 3500 ppm are immediately dangerous to life and health.</p>	<p>HEALTH Hazardous Substance</p>
<p>Skin Contact: Flood all areas of body that have contacted the substance with water. Don't wait to remove contaminated clothing; do it under the water stream. Use soap to help assure removal. Isolate contaminated clothing when removed to prevent contact by others.</p> <p>Eye Contact: Remove any contact lenses at once. Flush eyes well with copious quantities of water or normal saline for at least 20-30 minutes. Seek medical attention.</p> <p>Inhalation: Leave contaminated area immediately; breathe fresh air. Proper respiratory protection must be supplied to any rescuers. If coughing, difficult breathing or any other symptoms develop, seek medical attention at once, even if symptoms develop many hours after exposure.</p> <p>Ingestion: If convulsions are not present, give a glass or two of water or milk to dilute the substance. Assure that the person's airway is unobstructed and contact a hospital or poison center immediately for advice on whether or not to induce vomiting.</p>	<p>HAZARDOUS To the Environment</p>
<p>Storage Precautions: Store in a refrigerator and protect from oxidizers.</p> <p>Spills and Leakage: Use absorbent paper to pick up spilled material. Follow by washing surfaces well first with alcohol, then with soap and water. Seal all wastes in vapor-tight plastic bags for eventual disposal.</p> <p>Suggested Gloves: Not available</p> <p>Uses: Solvent, chemical intermediate for synthesis.</p> <p>Additional Reference Sources: <u>Dangerous Properties of Industrial Materials</u>, N. I. Sax, 5th Ed., p. 488 (1979), Van Nostrand Reinhold. <u>Patty's Industrial Hygiene and Toxicology</u>, G. C. Clayton and F. E. Clayton, 3rd Revised Ed., p. 3604 (1981), John Wiley and Sons. <u>Handbook of Chemistry and Physics</u>, R. Weast et al, 60th Ed., p. C-132 (1979), CRC Press.</p>	<p>HAZARDOUS To the Environment</p>

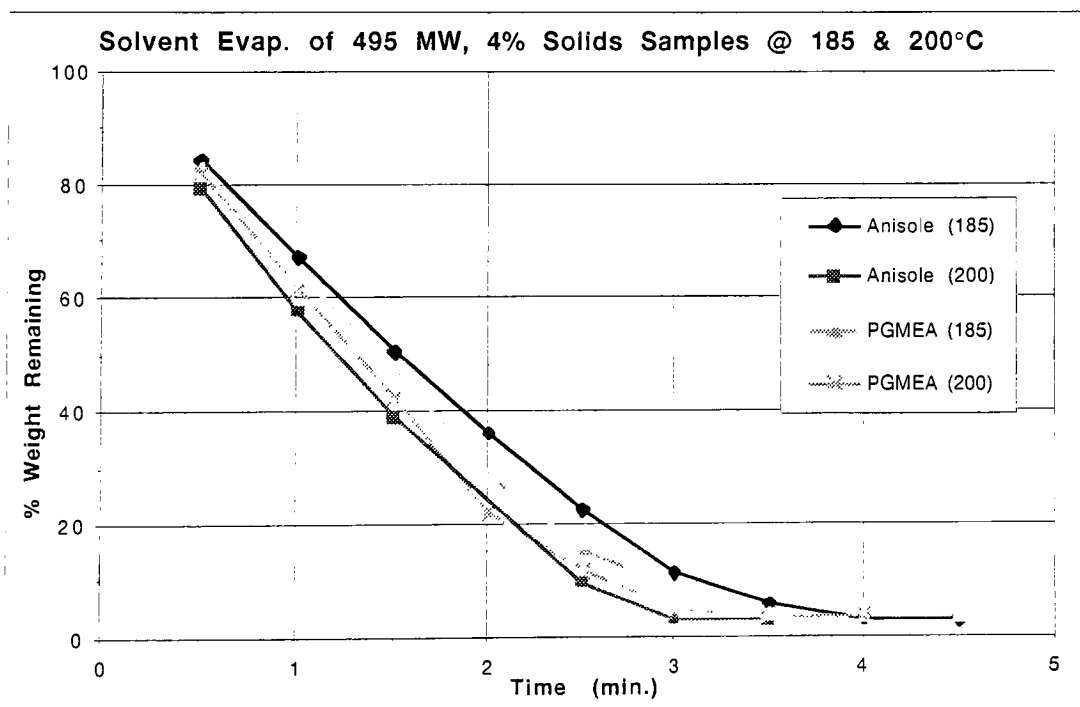
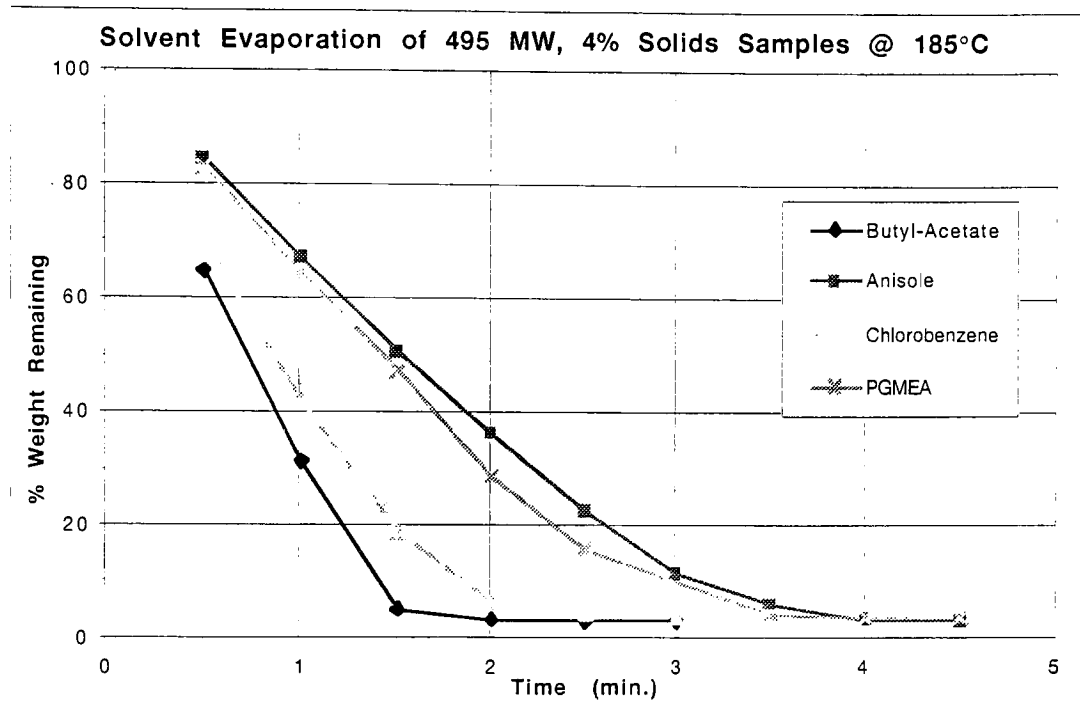
APPENDIX B

Solvent Evaporation Rate Characteristic Curves for Experimental Samples

Appendix B (Cont.)



Appendix B (Cont.)



APPENDIX C

Completed Experimental Data Sheets

Appendix C (Cont.)

C_4_1 - Experiment Worksheet

Run #	PreBake (C)	Dev. Time (s)	Eo (uC/cm^2)	Contrast	Resist Loss(Å)
1	180	60	64	5.07	5
2	160	45	67	4.93	3
3	170	60	62	5.15	0
4	180	30	75	5.54	17
5	170	45	68	5.58	14
6	160	60	60	4.76	0
7	170	45	67	5.48	3
8	170	30	75	5.97	20
9	160	30	72	5.49	8
10	180	45	67	5.07	5

C_4_2 - Experiment Worksheet

Run #	PreBake (C)	Dev. Time (s)	Eo (uC/cm^2)	Contrast	Resist Loss(Å)
1	170	45	65	5.58	1
2	180	45	63	4.44	8
3	180	60	57	4.05	0
4	180	30	70	5.78	0
5	160	30	70	5.58	15
6	160	45	63	5.36	0
7	170	60	60	4.98	7
8	170	45	65	5.57	0
9	160	60	60	4.76	0
10	170	30	70	6.1	32

C_4_3 - Experiment Worksheet

Run #	PreBake (C)	Dev. Time (s)	Eo (uC/cm^2)	Contrast	Resist Loss(Å)
1	170	45	65	5.27	0
2	160	60	58	5.23	8
3	180	30	75	5.59	45
4	170	45	66	5.47	13
5	160	30	72	5.68	10
6	160	45	67	5.48	10
7	180	60	63	4.8	19
8	180	45	70	5.05	24
9	170	60	61	5.15	5
10	170	30	73	5.97	8

C_4_4 - Experiment Worksheet

Run #	PreBake (C)	Dev. Time (s)	Eo (uC/cm^2)	Contrast	Resist Loss(Å)
1	160	45	68	5.78	0
2	180	45	68	5.12	3
3	170	45	70	6.08	1
4	170	45	69	5.78	0
5	180	60	63	4.8	8
6	160	30	73	5.98	0
7	180	30	76	5.25	2
8	160	60	63	5.57	0
9	170	60	65	5.57	0
10	170	30	74	6.29	0

Appendix C (Cont.)

C_4_C - Experiment Worksheet

Run #	PreBake (C)	Dev. Time (s)	Eo (uC/cm^2)	Contrast	Resist Loss(Å)
1	180	60	61	4.87	9
2	180	45	66	5.48	7
3	160	30	70	5.78	0
4	170	30	73	5.97	12
5	160	60	60	5.04	0
6	160	45	64	5.27	0
7	180	30	73	5.78	0
8	170	60	58	5.12	10
9	170	45	65	5.57	2
10	170	45	65	5.57	16

A_6 - Experiment Worksheet

Run #	PreBake (C)	Dev. Time (s)	Eo (uC/cm^2)	Contrast	Resist Loss(Å)
1	185	45	66	5.68	0
2	185	45	66	5.68	0
3	195	45	69	5.68	0
4	175	60	60	5.04	0
5	175	45	65	5.57	5
6	195	60	66	5.09	0
7	185	30	73	6.08	3
8	185	60	60	5.35	0
9	195	30	77	5.96	0
10	175	30	73	6.08	0

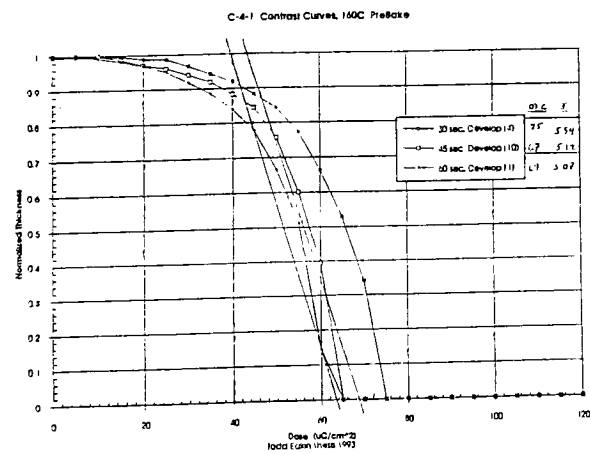
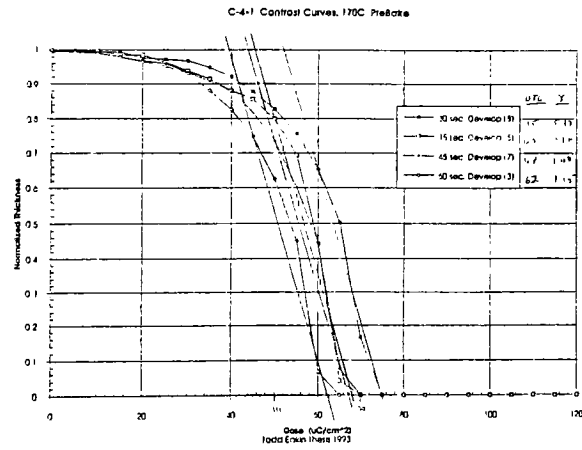
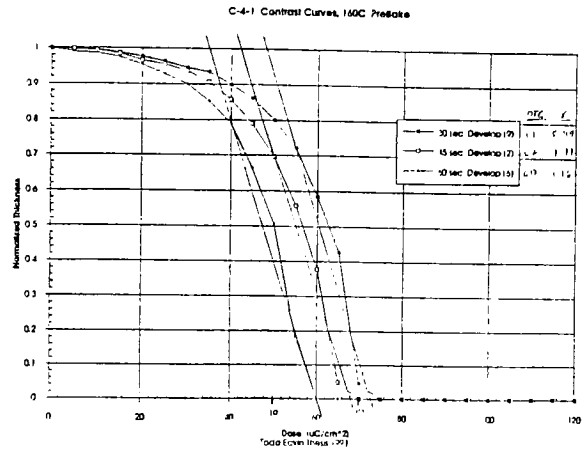
P_6 - Experiment Worksheet

Run #	PreBake (C)	Dev. Time (s)	Eo (uC/cm^2)	Contrast	Resist Loss(Å)
1	195	45	66	5.02	0
2	195	60	60	4.51	0
3	195	30	75	5.41	2
4	175	60	61	5.15	0
5	185	45	66	5.57	0
6	185	45	65	5.79	0
7	185	60	63	5.27	10
8	175	45	65	5.57	2
9	175	30	73	5.78	0
10	185	30	70	5.94	0

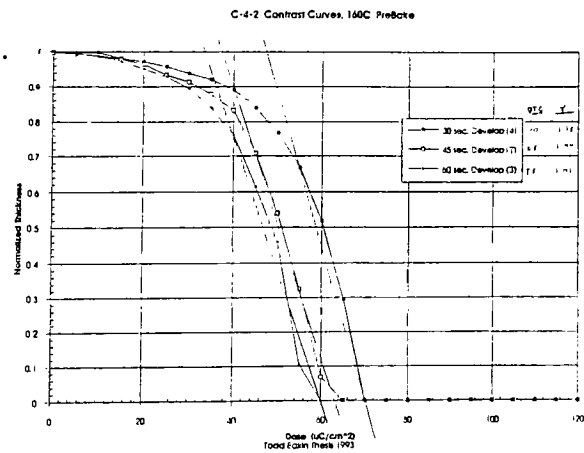
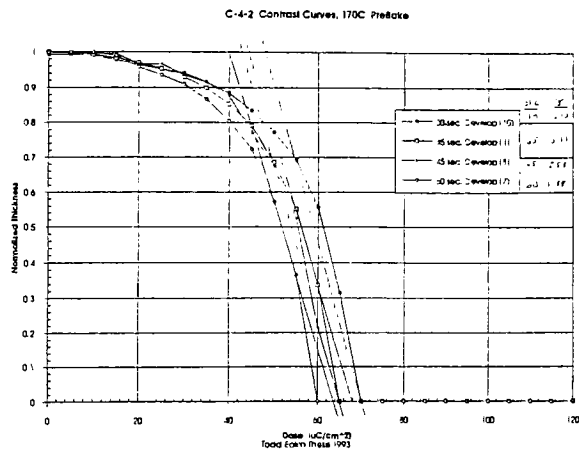
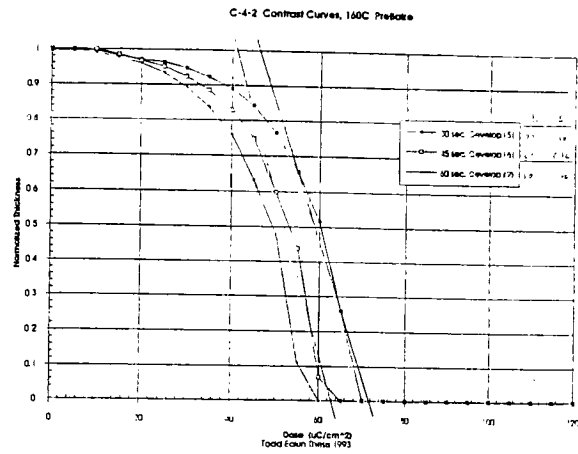
APPENDIX D

Experiential Output Contrast Curves

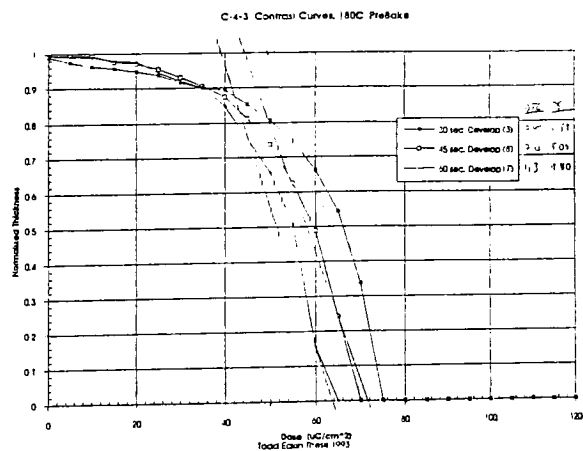
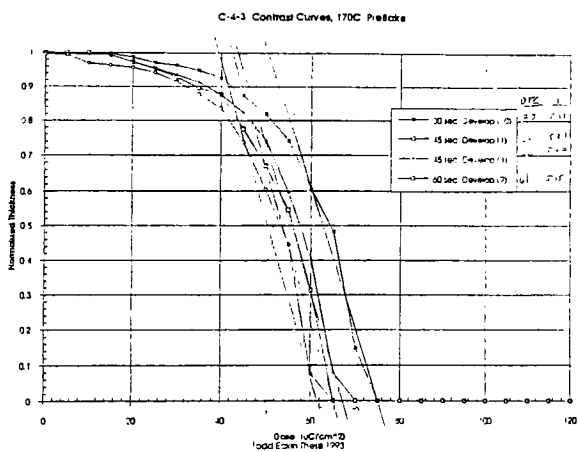
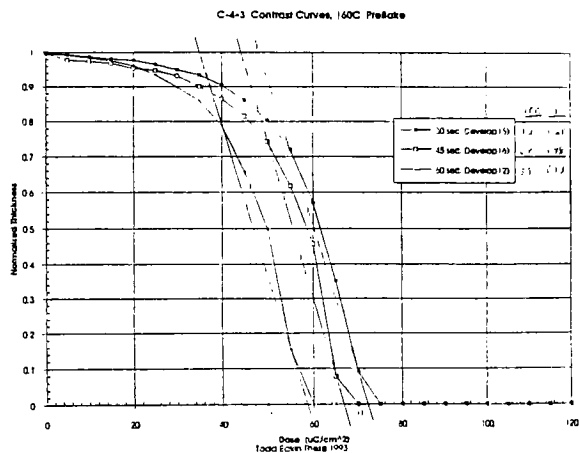
Appendix D (Cont.)



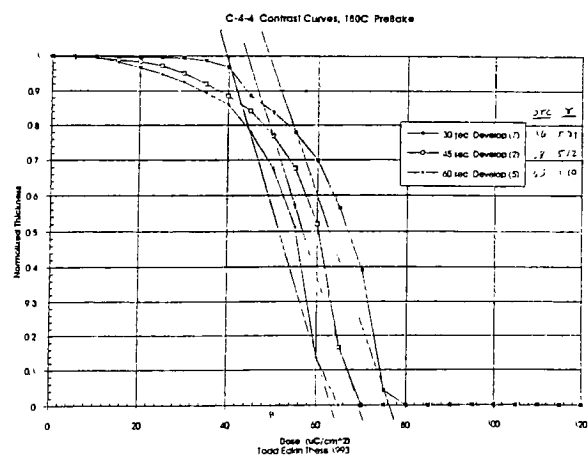
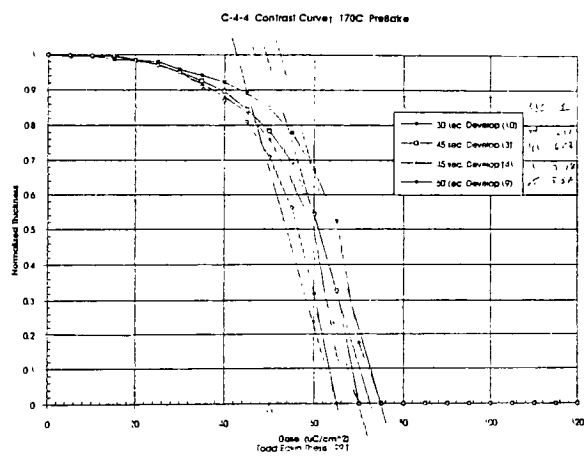
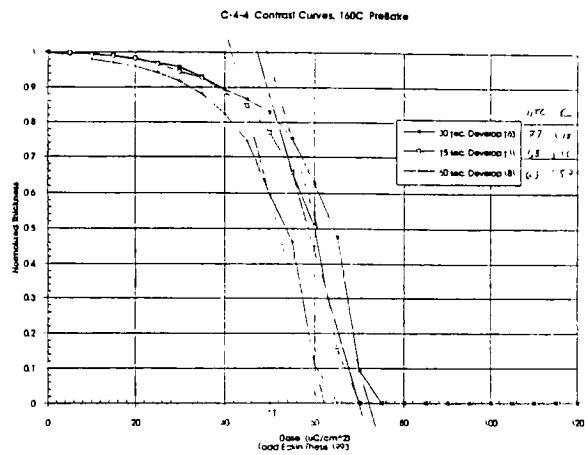
Appendix D (Cont.)



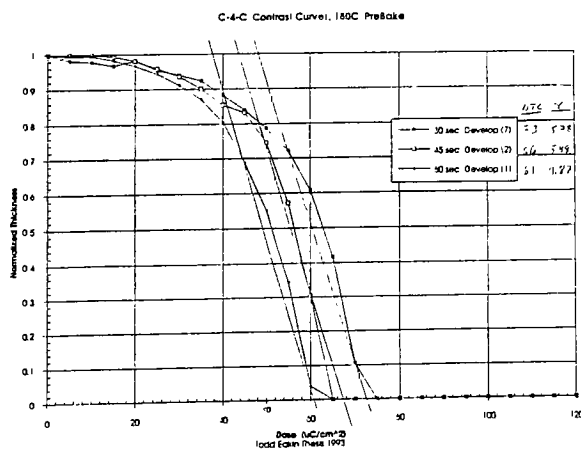
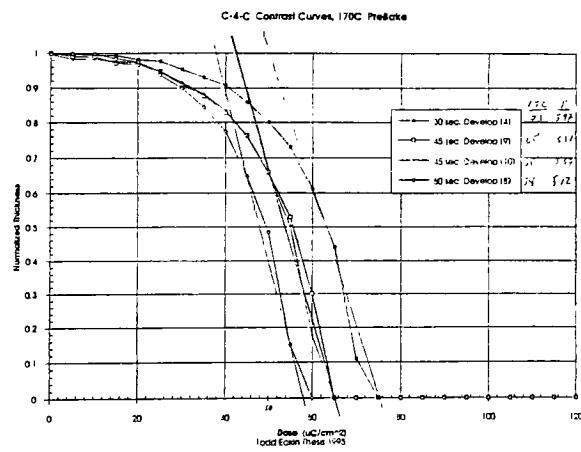
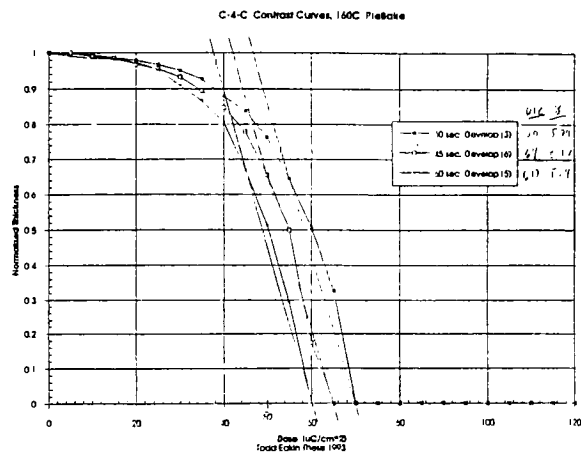
Appendix D (Cont.)



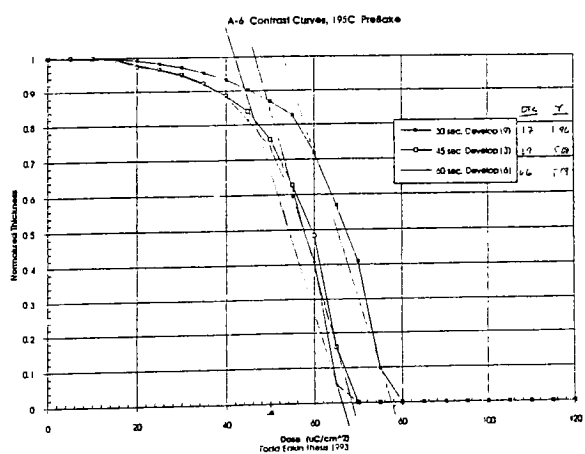
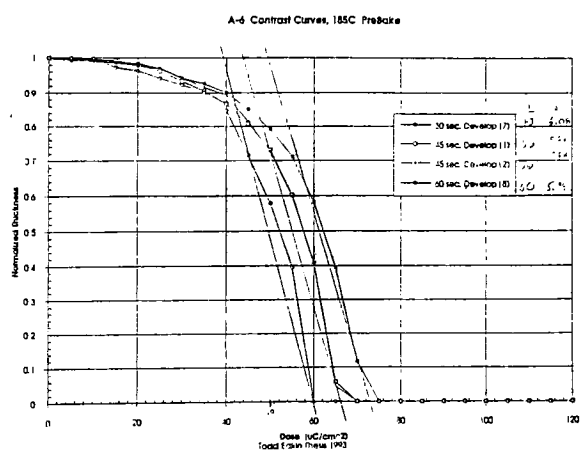
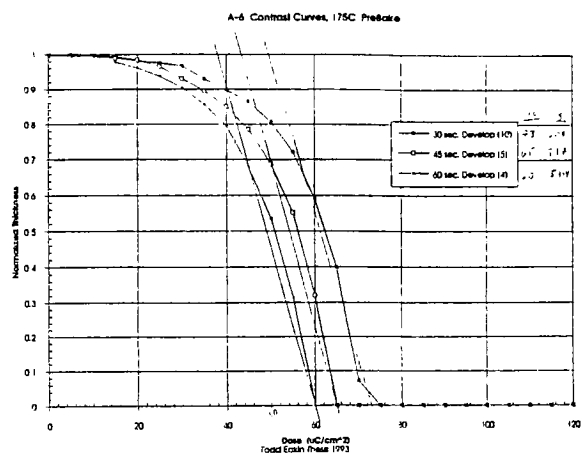
Appendix D (Cont.)



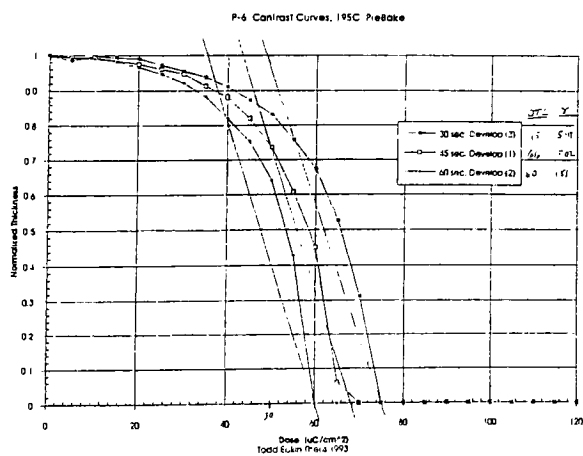
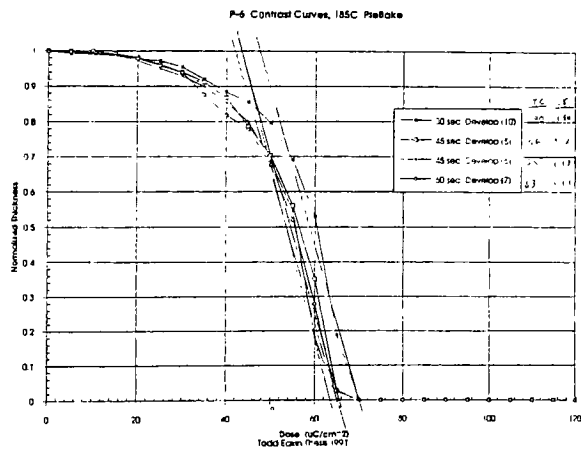
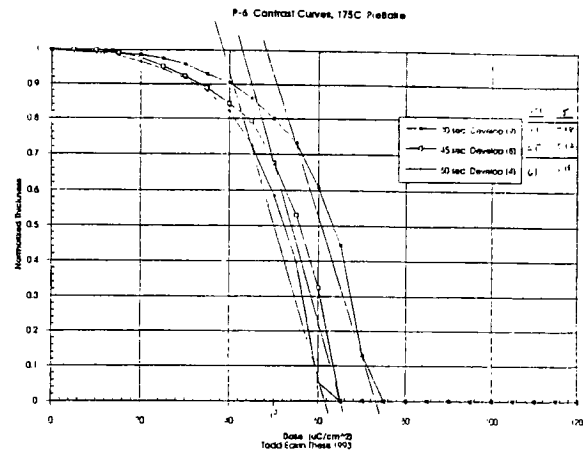
Appendix D (Cont.)



Appendix D (Cont.)



Appendix D (Cont.)

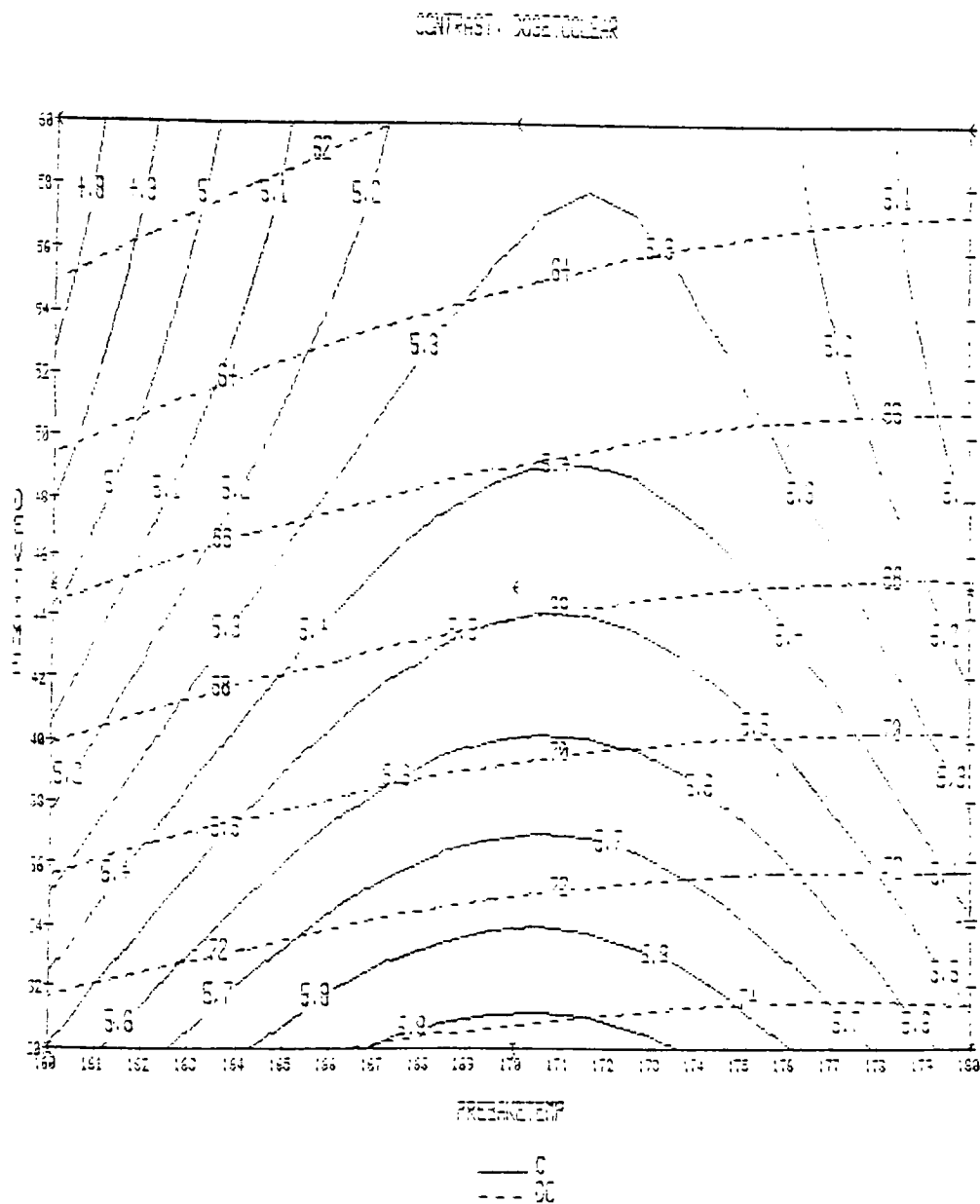


APPENDIX E

Experimental Output Contour Plots and Anova Tables

Appendix E (Cont.)

C-4-1 Contour Plot



Appendix E (Cont.)

ANOVA TABLES FOR SAMPLE C-4-1

Least Squares Summary ANOVA, Response DOSE TO CLEAR Model DESIGN

Source	df	Sum Sq.	Mean Sq.	F-ratio	Signif.
Total (Corr.)	9	232.1000			
Regression	5	226.7310	45.3462	33.78	0.0023
Linear	2	224.1667	112.0833	83.50	0.0005
Non-Linear	3	2.5643	0.0855	0.64	0.6297
Residual	4	5.3690	1.3423		
Lack of fit	3	4.8690	1.6230	3.25	0.3624
Pure error	1	0.5000	0.0500		
R-sq. = 0.9769					
R-sq-adj. = 0.9460					

Least Squares Summary ANOVA, Response CONTRAST Model DESIGN

Source	df	Sum Sq.	Mean Sq.	F-ratio	Signif.
Total (Corr.)	9	1.2100			
Regression	5	1.1666	0.2338	22.68	0.0049
Linear	2	0.7217	0.3609	35.02	0.0029
Non-Linear	3	0.4471	0.1490	14.46	0.0130
Residual	4	0.0412	0.0103		
Lack of fit	3	0.0362	0.0121	2.42	0.4343
Pure error	1	0.0050	0.0050		
R-sq. = 0.9659					
R-sq-adj. = 0.9233					

Least Squares Summary ANOVA, Response THICKNESS LOSS Model DESIGN

Source	df	Sum Sq.	Mean Sq.	F-ratio	Signif.
Total (Corr.)	9	454.5000			
Regression	5	350.0476	70.0095	2.66	0.1803
Linear	2	309.3333	154.6667	5.92	0.0637
Non-Linear	3	40.7143	13.5714	0.52	0.6912
Residual	4	104.4524	26.1131		
Lack of fit	3	43.9524	14.6506	0.24	0.6649
Pure error	1	60.5000	60.5000		
R-sq. = 0.7702					
R-sq-adj. = 0.4829					

Least Squares Components ANOVA, Response DOSE TO CLEAR Model DESIGN

Source	df	Sum Sq.	Mean Sq.	F-ratio	Signif.
Constant	1	4.5833			
Pre-Bake	1	8.1667	8.1667	6.06	0.0692
Dev-Time	1	216.0000	216.0000	160.90	0.0002
Pre-Bake^2	1	0.9643	0.9643	0.72	0.4444
P-B * D-T	1	0.2500	0.2500	0.19	0.6883
Dev-Time^2	1	1.7143	1.7143	1.28	0.3216
Residual	4	5.3690	1.3423		
R-sq. = 0.9769					
R-sq-adj. = 0.9480					

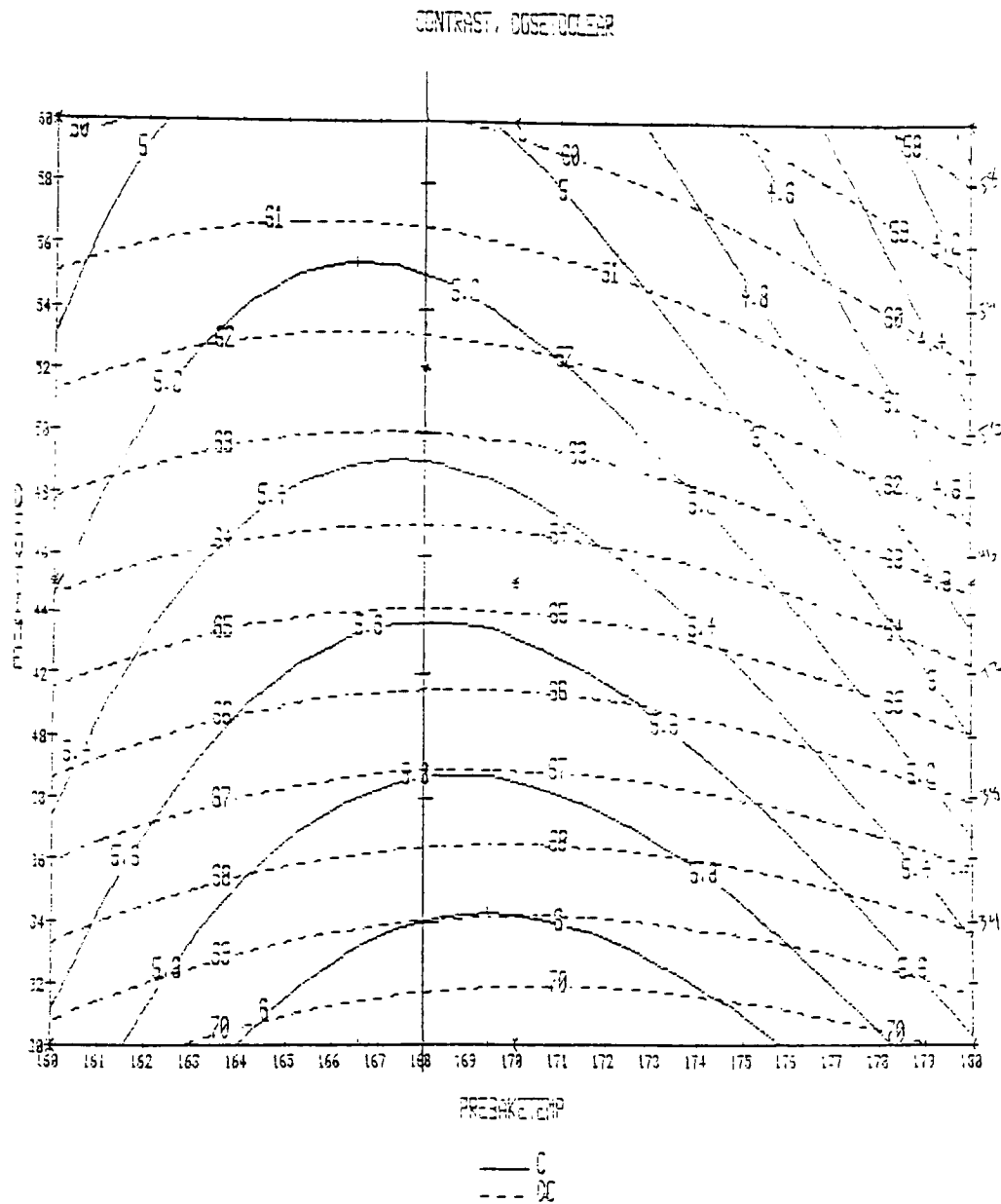
Least Squares Components ANOVA, Response CONTRAST Model DESIGN

Source	df	Sum Sq.	Mean Sq.	F-ratio	Signif.
Constant	1	261.0000			
Pre-Bake	1	0.0417	0.0417	4.04	0.1147
Dev-Time	1	0.6801	0.6801	65.99	0.0012
Pre-Bake^2	1	0.4200	0.4200	40.76	0.0031
P-B * D-T	1	0.0169	0.0169	1.64	0.2696
Dev-Time^2	1	0.0430	0.0429	4.17	0.1107
Residual	4	0.0412	0.0103		
R-sq. = 0.9659					
R-sq-adj. = 0.9233					

Least Squares Components ANOVA, Response THICKNESS LOSS Model DESIGN

Source	df	Sum Sq.	Mean Sq.	F-ratio	Signif.
Constant	1	562.5000			
Pre-Bake	1	42.6667	42.6667	1.63	0.2703
Dev-Time	1	266.6667	266.6667	10.21	0.0330
Pre-Bake^2	1	26.2976	26.2976	1.01	0.3724
P-B * D-T	1	4.0000	4.0000	0.15	0.7155
Dev-Time^2	1	16.2976	16.2976	0.62	0.4737
Residual	4	104.4524	26.1131		
R-sq. = 0.7702					
R-sq-adj. = 0.4829					

C-4-2 Contour Plot



Appendix E (Cont.)

ANOVA TABLES FOR SAMPLE C-4-2

Least Squares Summary ANOVA, Response DOSE TO CLEAR Model DESIGN					
Source	df	Sum Sq.	Mean Sq.	F-ratio	Signif.
Total (Corr.)	9	192.1000			
Regression	5	169.7071	37.9414	63.42	0.0007
Linear	2	163.0000	91.5000	153.00	0.0002
Non-Linear	3	6.7071	2.2357	3.74	0.1177
Residual	4	2.3929	0.5962		
Lack of fit	3	2.3929	0.7976		
Pure error	1	0.0000	0.0000		
R-sq. = 0.9675					
R-sq-adj. = 0.9720					

Least Squares Summary ANOVA, Response CONTRAST Model DESIGN					
Source	df	Sum Sq.	Mean Sq.	F-ratio	Signif.
Total (Corr.)	9	3.7356			
Regression	5	3.5623	0.7125	16.43	0.0090
Linear	2	2.5656	1.2926	29.61	0.0040
Non-Linear	3	0.9767	0.3256	7.51	0.0404
Residual	4	0.1735	0.0434		
Lack of fit	3	0.1734	0.0576	1156.00	0.0216
Pure error	1	0.0001	0.0001		
R-sq. = 0.9536					
R-sq-adj. = 0.6955					

Least Squares Summary ANOVA, Response THICKNESS LOSS Model DESIGN					
Source	df	Sum Sq.	Mean Sq.	F-ratio	Signif.
Total (Corr.)	9	966.1000			
Regression	5	571.6633	114.3367	1.16	0.4557
Linear	2	274.6333	137.4167	1.39	0.3473
Non-Linear	3	296.6500	96.9500	1.00	0.4777
Residual	4	394.4167	96.6042		
Lack of fit	3	393.9167	131.3056	262.60	0.0453
Pure error	1	0.5000	0.5000		
R-sq. = 0.5917					
R-sq-adj. = 0.0614					

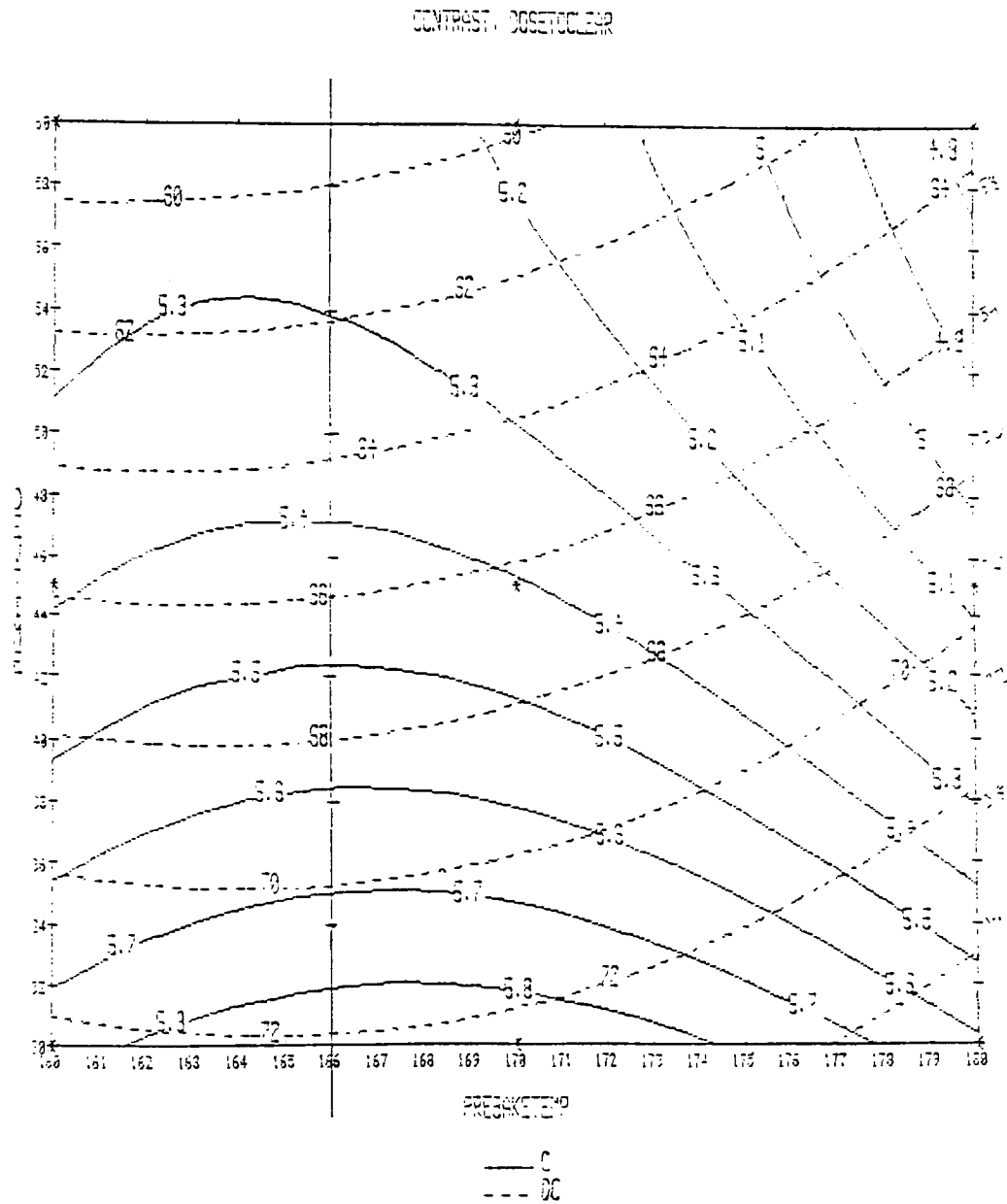
Least Squares Component ANOVA, Response DOSE TO CLEAR Model DESIGN					
Source	df	Sum Sq.	Mean Sq.	F-ratio	Signif.
Constant	1	41345.0000			
Pre-Bake	1	1.5000	1.5000	2.51	0.1665
Dev-Time	1	161.5000	161.5000	303.40	0.0001
Pre-Bake^2	1	3.6571	3.6571	6.45	0.0640
P-B * D-T	1	2.2500	2.2500	3.76	0.1245
Dev-Time^2	1	1.1905	1.1905	1.99	0.2312
Residual	4	2.3929	0.5962		
R-sq. = 0.9675					
R-sq-adj. = 0.9720					

Least Squares Component ANOVA, Response CONTRAST Model DESIGN					
Source	df	Sum Sq.	Mean Sq.	F-ratio	Signif.
Constant	1	727.0000			
Pre-Bake	1	0.3406	0.3406	7.66	0.0467
Dev-Time	1	2.2446	0.2446	51.76	0.0020
Pre-Bake^2	1	0.7676	0.7676	17.70	0.0136
P-B * D-T	1	0.2070	0.2070	4.77	0.0942
Dev-Time^2	1	0.0103	0.0103	0.24	0.6516
Residual	4	0.1735	0.0434		
R-sq. = 0.9536					
R-sq-adj. = 0.6955					

Least Squares Component ANOVA, Response THICKNESS LOSS Model DESIGN					
Source	df	Sum Sq.	Mean Sq.	F-ratio	Signif.
Constant	1	396.9000			
Pre-Bake	1	6.1667	6.1667	0.06	0.7676
Dev-Time	1	266.6667	266.6667	2.70	0.1754
Pre-Bake^2	1	131.2500	131.2500	1.33	0.3129
P-B * D-T	1	56.2500	56.2500	0.57	0.4921
Dev-Time^2	1	149.3333	149.3333	1.51	0.2659
Residual	4	394.4167	96.6042		
R-sq. = 0.5917					
R-sq-adj. = 0.0614					

Appendix E (Cont.)

C-4-3 Contour Plot



Appendix E (Cont.)

ANOVA TABLES FOR SAMPLE C-4-3

Least Squares Summary ANOVA, Response DOSE TO CLEAR Model DESIGN					
Source	df	Sum Sq.	Mean Sq.	F-ratio	Signif.
Total (Corr.)	9	272.0000			
Regression	5	265.6905	53.1381	33.69	0.0023
Linear	2	260.8333	130.4167	82.66	0.0006
Non-Linear	3	4.8571	1.6190	1.03	0.4700
Residual	4	6.3095	1.5774		
Lack of fit	3	5.8095	1.9365	3.87	0.3536
Pure error	1	0.5000	0.5000		
R-sq. = 0.9768					
R-sq-adj. = 0.9478					

Least Squares Summary ANOVA, Response CONTRAST Model DESIGN					
Source	df	Sum Sq.	Mean Sq.	F-ratio	Signif.
Total (Corr.)	9	1.0319			
Regression	5	0.9793	0.1959	14.89	0.0106
Linear	2	0.6577	0.4288	32.60	0.0033
Non-Linear	3	0.0122	0.0405	3.08	0.1528
Residual	4	0.0526	0.0132		
Lack of fit	3	0.0326	0.0109	0.05	0.7319
Pure error	1	0.0200	0.0200		
R-sq. = 0.9490					
R-sq-adj. = 0.8653					

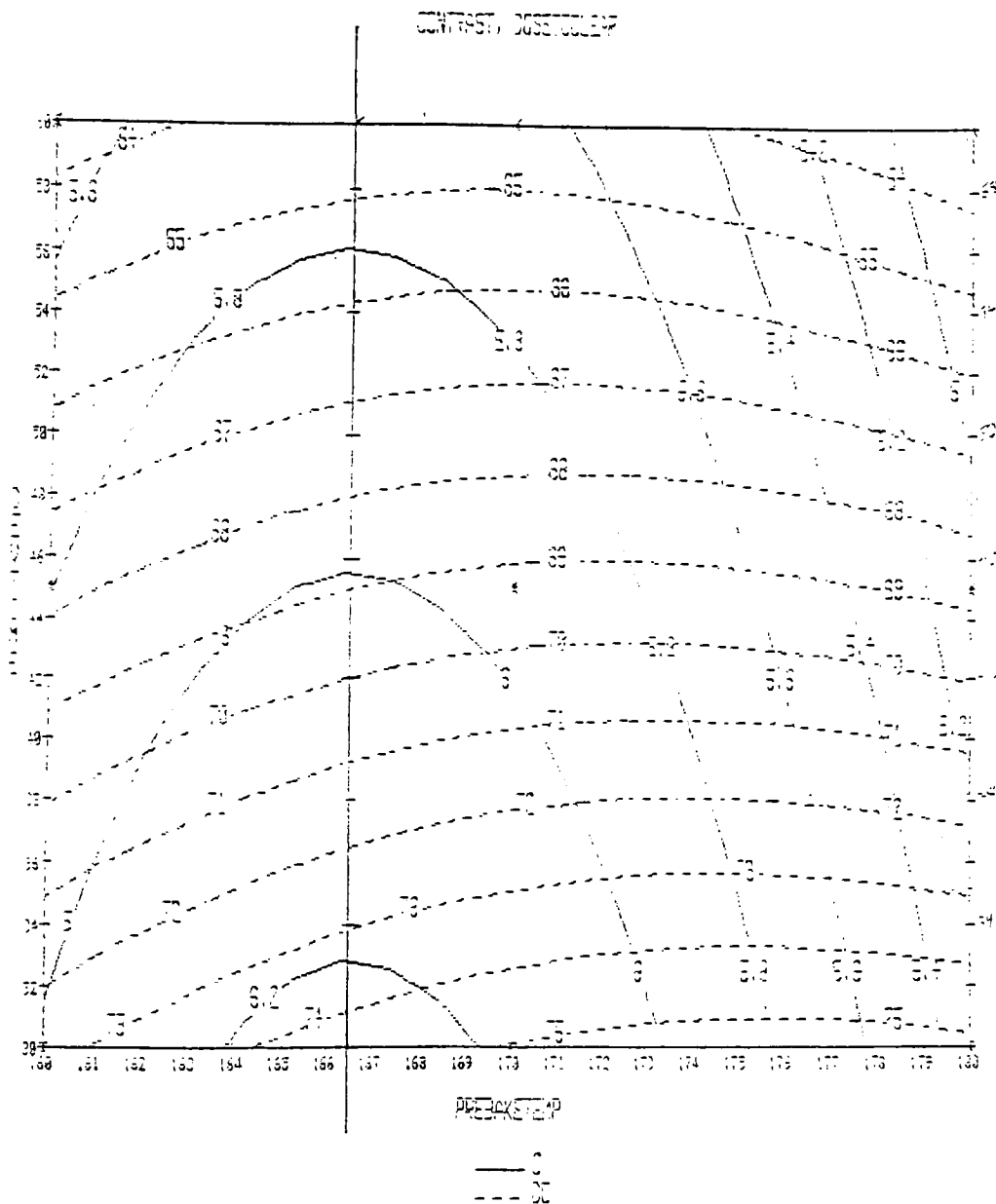
Least Squares Summary ANOVA, Response THICKNESS LOSS Model DESIGN					
Source	df	Sum Sq.	Mean Sq.	F-ratio	Signif.
Total (Corr.)	9	1467.6000			
Regression	5	1308.7670	261.7530	6.59	0.0458
Linear	2	760.1670	380.0830	9.57	0.0299
Non-Linear	3	548.6000	162.8670	4.61	0.0671
Residual	4	156.6330	39.7080		
Lack of fit	3	74.3330	24.7780	0.29	0.8380
Pure error	1	84.5000	84.5000		
R-sq. = 0.8916					
R-sq-adj. = 0.7565					

Least Squares Component ANOVA, Response DOSE TO CLEAR Model DESIGN					
Source	df	Sum Sq.	Mean Sq.	F-ratio	Signif.
Constant	1	44890.0000			
Pre-Bake	1	20.1667	20.1667	12.76	0.0233
Dev-Time	1	240.6667	240.6667	152.60	0.0002
Pre-Bake^2	1	3.6571	3.6571	2.45	0.1929
P-B * D-T	1	1.0000	1.0000	0.63	0.4705
Dev-Time^2	1	0.1071	0.1071	0.07	0.8073
Residual	4	6.3095	1.5774		
R-sq. = 0.9768					
R-sq-adj. = 0.9478					

Least Squares Component ANOVA, Response CONTRAST Model DESIGN					
Source	df	Sum Sq.	Mean Sq.	F-ratio	Signif.
Constant	1	288.0000			
Pre-Bake	1	0.1504	0.1504	11.43	0.0278
Dev-Time	1	0.7073	0.7073	53.76	0.0018
Pre-Bake^2	1	0.0750	0.0750	5.70	0.0754
P-B * D-T	1	0.0289	0.0289	2.20	0.2124
Dev-Time^2	1	0.0312	0.0312	2.36	0.1982
Residual	4	0.0526	0.0132		
R-sq. = 0.9490					
R-sq-adj. = 0.8653					

Least Squares Component ANOVA, Response THICKNESS LOSS Model DESIGN					
Source	df	Sum Sq.	Mean Sq.	F-ratio	Signif.
Constant	1	2016.4000			
Pre-Bake	1	600.0000	600.0000	15.11	0.0177
Dev-Time	1	160.1670	160.1670	4.03	0.1150
Pre-Bake^2	1	364.5830	364.5830	9.18	0.0388
P-B * D-T	1	144.0000	144.0000	3.63	0.1296
Dev-Time^2	1	9.3330	9.3330	0.24	0.6532
Residual	4	158.8330	39.7080		
R-sq. = 0.8918					
R-sq-adj. = 0.7565					

C-4-4 Contour Plot



Appendix E (Cont.)

ANOVA TABLES FOR SAMPLE C-4-4

Least Squares Summary ANOVA, Response DOSE TO CLEAR Model DESIGN					
Source	df	Sum Sq.	Mean Sq.	F-ratio	Signif.
Total (Corr.)	9	180.9000			
Regression	5	177.2452	35.4490	38.80	0.0018
Linear	2	172.1667	86.0833	94.21	0.0004
Non-Linear	3	5.0786	1.6929	1.85	0.2782
Residual	4	3.6548	0.9137		
Lack of fit	3	3.1548	1.0516	2.10	0.4600
Pure error	1	0.5000	0.5000		
R-sq. = 0.9798					
R-sq-adj. = 0.9545					

Least Squares Summary ANOVA, Response CONTRAST Model DESIGN					
Source	df	Sum Sq.	Mean Sq.	F-ratio	Signif.
Total (Corr.)	9	1.9056			
Regression	5	1.8284	0.3657	18.96	0.0069
Linear	2	1.1937	0.5968	30.94	0.0037
Non-Linear	3	0.6347	0.2116	10.97	0.0212
Residual	4	0.0772	0.0193		
Lack of fit	3	0.0322	0.0107	0.24	0.8671
Pure error	1	0.0450	0.0450		
R-sq. = 0.9595					
R-sq-adj. = 0.9089					

Least Squares Summary ANOVA, Response THICKNESS LOSS Model DESIGN					
Source	df	Sum Sq.	Mean Sq.	F-ratio	Signif.
Total (Corr.)	9	38.4000			
Regression	5	52.2810	10.4562	6.84	0.0431
Linear	2	34.1667	17.0833	11.17	0.0231
Non-Linear	3	18.1143	6.0381	3.95	0.1090
Residual	4	6.1191	1.5298		
Lack of fit	3	5.6191	1.8730	3.75	0.3589
Pure error	1	0.5000	0.5000		
R-sq. = 0.8952					
R-sq-adj. = 0.7642					

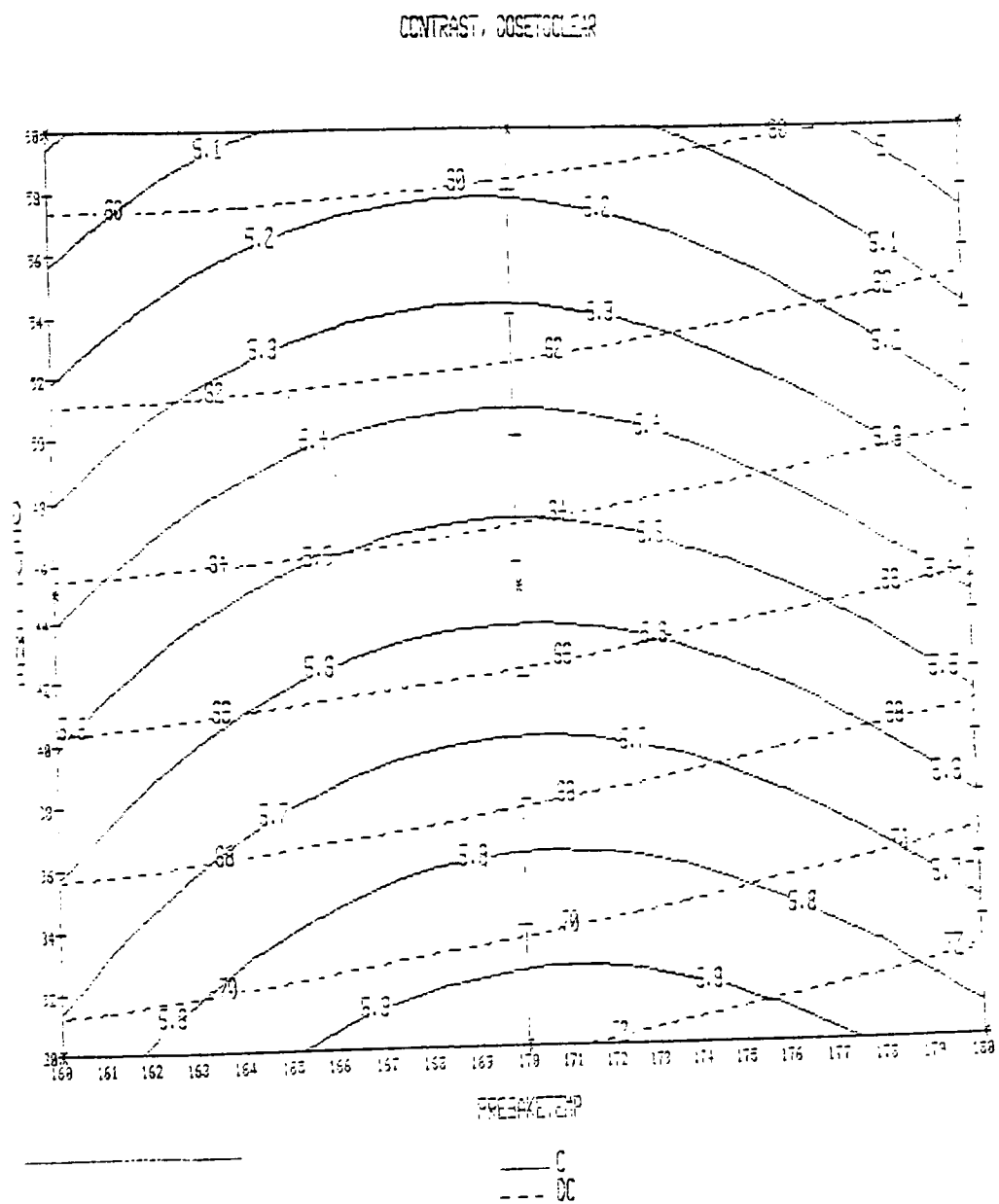
Least Squares Component ANOVA, Response DOSE TO CLEAR Model DESIGN					
Source	df	Sum Sq.	Mean Sq.	F-ratio	Signif.
Constant	1	47472.0000			
Pre-Bake	1	1.5000	1.5000	1.64	0.2693
Dev-Time	1	170.6867	170.6867	186.80	0.0002
Pre-Bake^2	1	2.6786	2.6786	2.93	0.1620
P-B * D-T	1	2.2500	2.2500	2.46	0.1917
Dev-Time^2	1	0.4288	0.4288	0.47	0.5310
Residual	4	3.8548	0.9137		
R-sq. = 0.9798					
R-sq-adj. = 0.9545					

Least Squares Component ANOVA, Response CONTRAST Model DESIGN					
Source	df	Sum Sq.	Mean Sq.	F-ratio	Signif.
Constant	1	316.0000			
Pre-Bake	1	0.7776	0.7776	40.31	0.0032
Dev-Time	1	0.4161	0.4161	21.57	0.0097
Pre-Bake^2	1	0.6035	0.6035	31.29	0.0050
P-B * D-T	1	0.0004	0.0004	0.02	0.8925
Dev-Time^2	1	0.0019	0.0019	0.10	0.7691
Residual	4	0.0772	0.0193		
R-sq. = 0.9595					
R-sq-adj. = 0.9089					

Least Squares Component ANOVA, Response THICKNESS LOSS Model DESIGN					
Source	df	Sum Sq.	Mean Sq.	F-ratio	Signif.
Constant	1	19.6000			
Pre-Bake	1	28.1667	28.1667	18.41	0.0127
Dev-Time	1	6.0000	6.0000	3.92	0.1187
Pre-Bake^2	1	8.0476	8.0476	5.26	0.0835
P-B * D-T	1	9.0000	9.0000	5.88	0.0723
Dev-Time^2	1	0.2976	0.2976	0.19	0.8819
Residual	4	6.1191	1.5298		
R-sq. = 0.8952					
R-sq-adj. = 0.7642					

Appendix E (Cont.)

C-4-C Contour Plot



Appendix E (Cont.)

ANOVA TABLES FOR SAMPLE C-4-C

Least Squares Summary ANOVA, Response DOSE TO CLEAR Model DESIGN					
Source	df	Sum Sq.	Mean Sq.	F-ratio	Signif.
Total (Corr.)	9	242.5000			
Regression	5	237.0238	47.4048	34.63	0.0022
Linear	2	234.1667	117.0833	85.52	0.0005
Non-Linear	3	2.8571	0.9524	0.70	0.6014
Residual	4	5.4762	1.3690		
Lack of fit	3	5.4762	1.8254		
Pure error	1	0.0000	0.0000		
R-sq. = 0.9774					
R-sq-adj. = 0.9492					

Least Squares Summary ANOVA, Response CONTRAST Model DESIGN					
Source	df	Sum Sq.	Mean Sq.	F-ratio	Signif.
Total (Corr.)	9	1.1635			
Regression	5	1.1341	0.2268	30.87	0.0027
Linear	2	1.0419	0.5210	70.90	0.0008
Non-Linear	3	0.0921	0.0307	4.18	0.1004
Residual	4	0.0294	0.0073		
Lack of fit	3	0.0294	0.0098		
Pure error	1	0.0000	0.0000		
R-sq. = 0.9747					
R-sq-adj. = 0.9432					

Least Squares Summary ANOVA, Response THICKNESS LOSS Model DESIGN					
Source	df	Sum Sq.	Mean Sq.	F-ratio	Signif.
Total (Corr.)	9	320.4000			
Regression	5	200.1976	40.0395	1.33	
Linear	2	50.8333	25.4167	0.85	0.4019
Non-Linear	3	149.3643	49.7881	1.66	0.4939
Residual	4	120.2024	30.0506		0.3117
Lack of fit	3	22.2024	7.4008	0.08	0.9642
Pure error	1	98.0000	98.0000		
R-sq. = 0.6248					
R-sq-adj. = 0.1559					

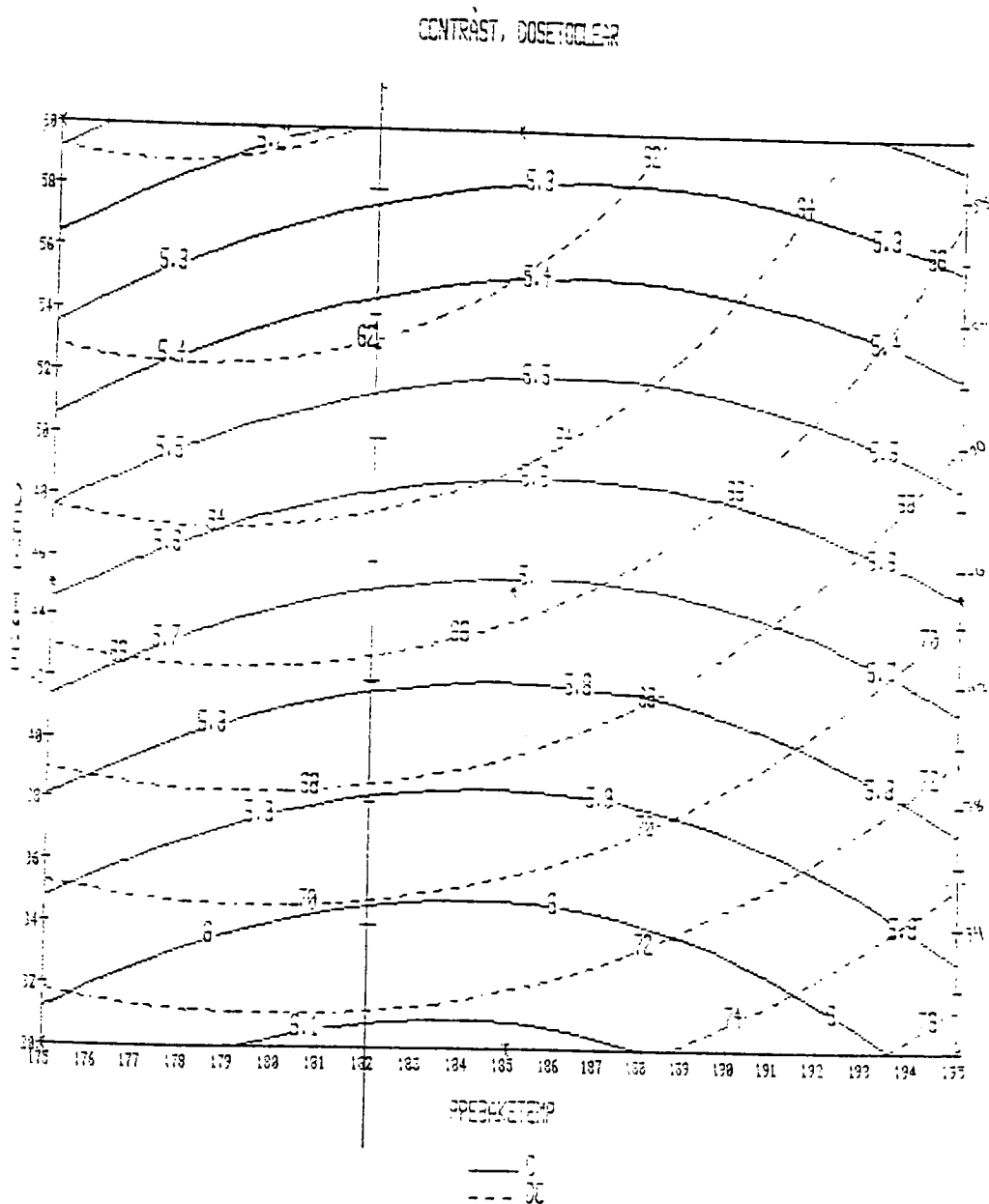
Least Squares Component ANOVA, Response DOSE TO CLEAR Model DESIGN					
Source	df	Sum Sq.	Mean Sq.	F-ratio	Signif.
Constant	1	42903.0000			
Pre-Bake	1	6.0000	6.0000	4.38	0.1044
Dev-Time	1	228.1667	228.1667	166.70	0.0002
Pre-Bake^2	1	0.1905	0.1905	0.14	0.7281
P-B * D-T	1	1.0000	1.0000	0.73	0.4409
Dev-Time^2	1	1.4405	1.4405	1.05	0.3630
Residual	4	5.4762	1.3690		
R-sq. = 0.9774					
R-sq-adj. = 0.9492					

Least Squares Component ANOVA, Response CONTRAST Model DESIGN					
Source	df	Sum Sq.	Mean Sq.	F-ratio	Signif.
Constant	1	296.0000			
Pre-Bake	1	0.0003	0.0003	0.04	0.8582
Dev-Time	1	1.0417	1.0417	141.80	0.0003
Pre-Bake^2	1	0.0799	0.0799	10.87	0.0300
P-B * D-T	1	0.0072	0.0072	0.98	0.3775
Dev-Time^2	1	0.0005	0.0005	0.07	0.8250
Residual	4	0.0294	0.0073		
R-sq. = 0.9747					
R-sq-adj. = 0.9432					

Least Squares Component ANOVA, Response THICKNESS LOSS Model DESIGN					
Source	df	Sum Sq.	Mean Sq.	F-ratio	Signif.
Constant	1	313.6000			
Pre-Bake	1	42.6667	42.6667	1.42	0.2993
Dev-Time	1	8.1667	8.1667	0.27	0.6297
Pre-Bake^2	1	126.2976	126.2976	4.20	0.1097
P-B * D-T	1	20.2500	20.2500	0.67	0.4578
Dev-Time^2	1	0.0476	0.0476	0.00	0.9702
Residual	4	120.2024	30.0506		
R-sq. = 0.6248					
R-sq-adj. = 0.1559					

Appendix E (Cont.)

A-6 Contour Plot



Appendix E (Cont.)

ANOVA TABLES FOR SAMPLE A-6

Least Squares Summary ANOVA, Response DOSE TO CLEAR Model DESIGN					
Source	df	Sum Sq.	Mean Sq.	F-ratio	Signif.
Total (Corr.)	9	278.5000			
Regression	5	276.5476	55.3095	113.30	0.0002
Linear	2	260.6333	130.4167	267.20	0.0001
Non-Linear	3	15.7143	5.2361	10.73	0.0220
Residual	4	1.9524	0.4661		
Lack of fit	3	1.9524	0.6506		
Pure error	1	0.0000	0.0000		
R-sq. = 0.9930					
R-sq-adj. = 0.9642					

Least Squares Summary ANOVA, Response CONTRAST Model DESIGN					
Source	df	Sum Sq.	Mean Sq.	F-ratio	Signif.
Total (Corr.)	9	1.2423			
Regression	5	1.2105	0.2421	30.46	0.0026
Linear	2	1.1619	0.5809	73.14	0.0007
Non-Linear	3	0.0467	0.0162	2.04	0.2507
Residual	4	0.0316	0.0079		
Lack of fit	3	0.0316	0.0106		
Pure error	1	0.0000	0.0000		
R-sq. = 0.9744					
R-sq-adj. = 0.9425					

Least Squares Summary ANOVA, Response THICKNESS LOSS Model DESIGN					
Source	df	Sum Sq.	Mean Sq.	F-ratio	Signif.
Total (Corr.)	9	27.6000			
Regression	5	7.1236	1.4246	0.26	0.9034
Linear	2	5.6667	2.8333	0.55	0.6135
Non-Linear	3	1.4571	0.4657	0.09	0.9569
Residual	4	20.4762	5.1191		
Lack of fit	3	20.4762	6.8254		
Pure error	1	0.0000	0.0000		
R-sq. = 0.2561					
R-sq-adj. = 0.6693					

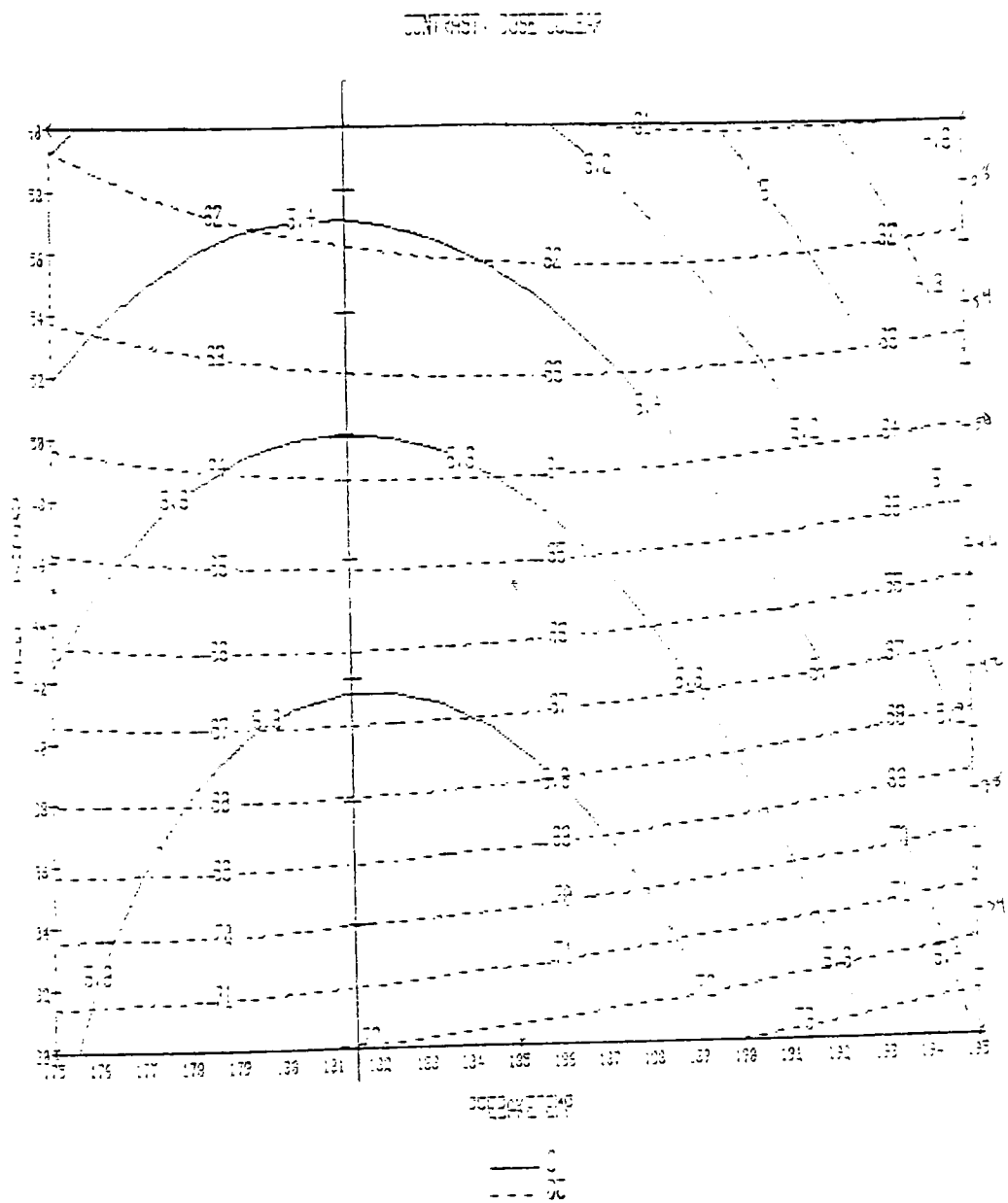
Least Squares Component ANOVA, Response DOSE TO CLEAR Model DESIGN					
Source	df	Sum Sq.	Mean Sq.	F-ratio	Signif.
Constant	1	45563.0000			
Pre-Bake	1	32.6667	32.6667	66.93	0.0012
Dev-Time	1	226.1667	226.1667	467.50	0.0000
Pre-Bake^2	1	6.0476	6.0476	16.49	0.0153
P-B * D-T	1	1.0000	1.0000	2.05	0.2256
Dev-Time^2	1	4.2976	4.2976	6.61	0.0413
Residual	4	1.9524	0.4661		
R-sq. = 0.9930					
R-sq-adj. = 0.9642					

Least Squares Component ANOVA, Response CONTRAST Model DESIGN					
Source	df	Sum Sq.	Mean Sq.	F-ratio	Signif.
Constant	1	316.0000			
Pre-Bake	1	0.0003	0.0003	0.03	0.6635
Dev-Time	1	1.1616	1.1616	146.20	0.0003
Pre-Bake^2	1	0.0346	0.0346	4.36	0.1044
P-B * D-T	1	0.0072	0.0072	0.91	0.3942
Dev-Time^2	1	0.0024	0.0024	0.30	0.6110
Residual	4	0.0316	0.0079		
R-sq. = 0.9744					
R-sq-adj. = 0.9425					

Least Squares Component ANOVA, Response THICKNESS LOSS Model DESIGN					
Source	df	Sum Sq.	Mean Sq.	F-ratio	Signif.
Constant	1	6.4000			
Pre-Bake	1	4.1667	4.1667	0.61	0.4160
Dev-Time	1	1.5000	1.5000	0.29	0.6170
Pre-Bake^2	1	0.1071	0.1071	0.02	0.6910
P-B * D-T	1	0.0000	0.0000	0.00	1.0000
Dev-Time^2	1	1.4405	1.4405	0.26	0.6239
Residual	4	20.4762	5.1191		
R-sq. = 0.2561					
R-sq-adj. = -0.6693					

Appendix E (Cont.)

P-6 Contour Plot



Appendix E (Cont.)

ANOVA TABLES FOR SAMPLE P-6

Least Squares Summary ANOVA, Response DOSE TO CLEAR Model DESIGN					
Source	df	Sum Sq.	Mean Sq.	F-ratio	Signif.
Total (Corr.)	9	216.4000			
Regression	5	201.4119	40.2824	10.75	0.0196
Linear	2	193.3330	96.6667	25.60	0.0052
Non-Linear	3	8.0766	2.6929	0.72	0.5907
Residual	4	14.9861	3.7470		
Lack of fit	3	14.4661	4.8294	9.66	0.2313
Pure error	1	0.5000	0.5000		
R-sq. = 0.9307					
R-sq-adj. = 0.6442					

Least Squares Summary ANOVA, Response CONTRAST Model DESIGN					
Source	df	Sum Sq.	Mean Sq.	F-ratio	Signif.
Total (Corr.)	9	1.6619			
Regression	5	1.6340	0.3266	46.63	0.0012
Linear	2	1.2123	0.6061	66.65	0.0005
Non-Linear	3	0.4217	0.1406	20.14	0.0071
Residual	4	0.0279	0.0070		
Lack of fit	3	0.0037	0.0012	0.05	0.9765
Pure error	1	0.0242	0.0242		
R-sq. = 0.9632					
R-sq-adj. = 0.9622					

Least Squares Summary ANOVA, Response THICKNESS LOSS Model DESIGN					
Source	df	Sum Sq.	Mean Sq.	F-ratio	Signif.
Total (Corr.)	9	88.4000			
Regression	5	27.7610	5.5562	0.37	0.6497
Linear	2	10.6667	5.3333	0.35	0.7231
Non-Linear	3	17.1143	5.7046	0.36	0.7759
Residual	4	60.6191	15.1546		
Lack of fit	3	60.6191	20.2064		
Pure error	1	0.0000	0.0000		
R-sq. = 0.3143					
R-sq-adj. = -0.5429					

Least Squares Component ANOVA, Response DOSE TO CLEAR Model DESIGN					
Source	df	Sum Sq.	Mean Sq.	F-ratio	Signif.
Constant	1	44090.0000			
Pre-Bake	1	0.6667	0.6667	0.16	0.6949
Dev-Time	1	192.6667	192.6667	51.42	0.0020
Pre-Bake^2	1	0.4266	0.4266	0.11	0.7522
P-B * D-T	1	2.2500	2.2500	0.60	0.4617
Dev-Time^2	1	4.7619	4.7619	1.27	0.3227
Residual	4	14.9661	3.7470		
R-sq. = 0.9307					
R-sq-adj. = 0.6442					

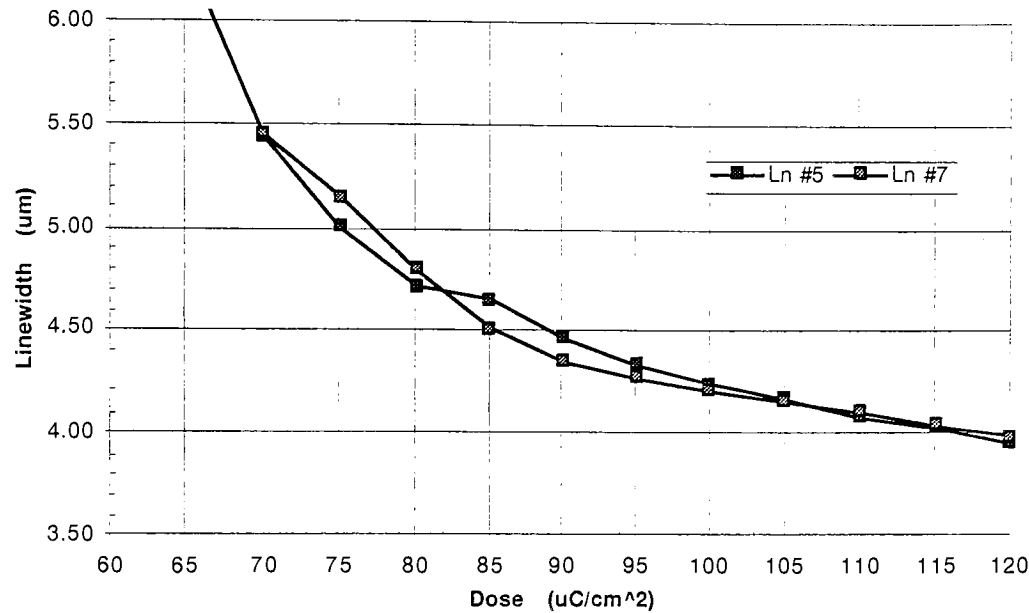
Least Squares Component ANOVA, Response CONTRAST Model DESIGN					
Source	df	Sum Sq.	Mean Sq.	F-ratio	Signif.
Constant	1	292.0000			
Pre-Bake	1	0.4056	0.4056	56.12	0.0016
Dev-Time	1	0.6067	0.6067	115.60	0.0004
Pre-Bake^2	1	0.3536	0.3536	50.67	0.0021
P-B * D-T	1	0.0162	0.0162	2.61	0.1614
Dev-Time^2	1	0.0147	0.0147	2.10	0.2207
Residual	4	0.0279	0.0070		
R-sq. = 0.9632					
R-sq-adj. = 0.9622					

Least Squares Component ANOVA, Response THICKNESS LOSS Model DESIGN					
Source	df	Sum Sq.	Mean Sq.	F-ratio	Signif.
Constant	1	19.6000			
Pre-Bake	1	0.0000	0.0000	0.00	1.0000
Dev-Time	1	10.6667	10.6667	0.70	0.4467
Pre-Bake^2	1	10.7143	10.7143	0.71	0.4476
P-B * D-T	1	1.0000	1.0000	0.07	0.6099
Dev-Time^2	1	6.0476	6.0476	0.53	0.5065
Residual	4	60.6191	15.1546		
R-sq. = 0.3143					
R-sq-adj. = -0.5429					

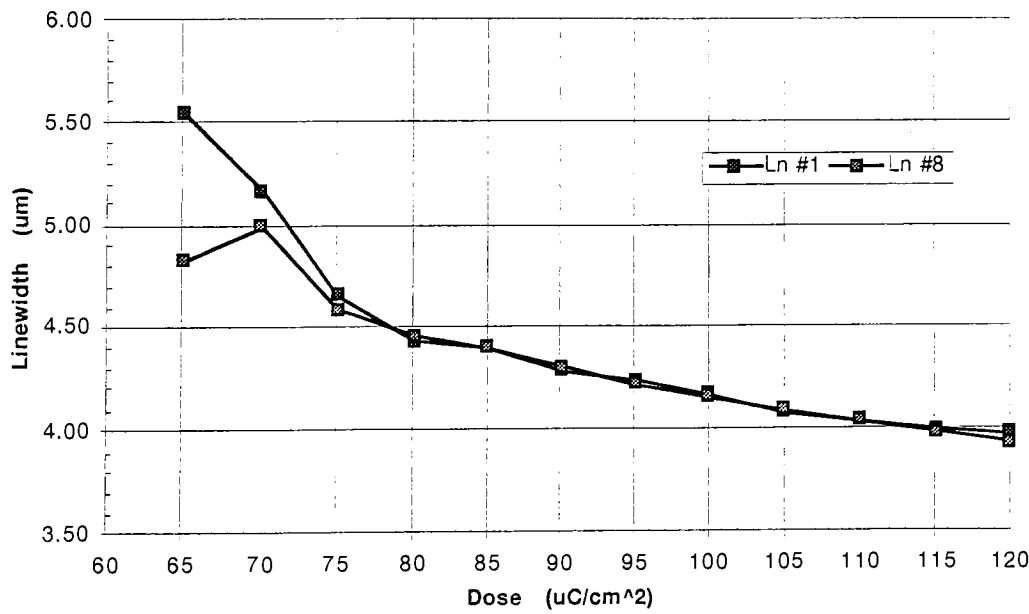
APPENDIX F

Experimental Linewidth Dimension Plots

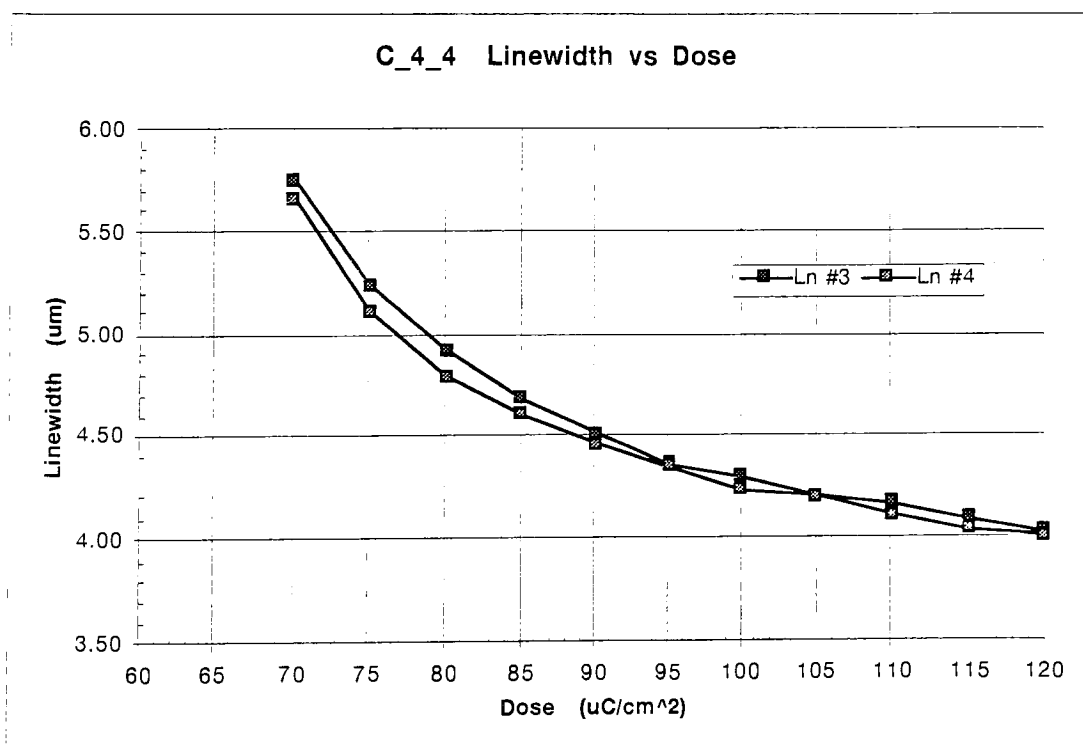
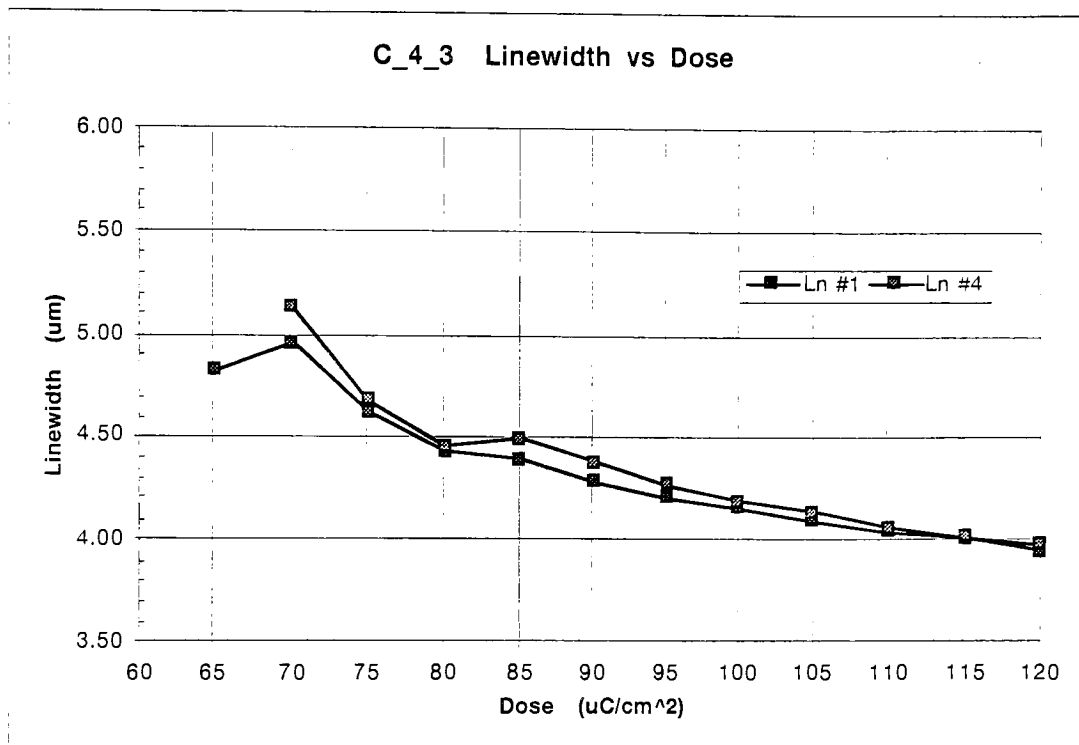
C_4_1 Linewidth vs Dose



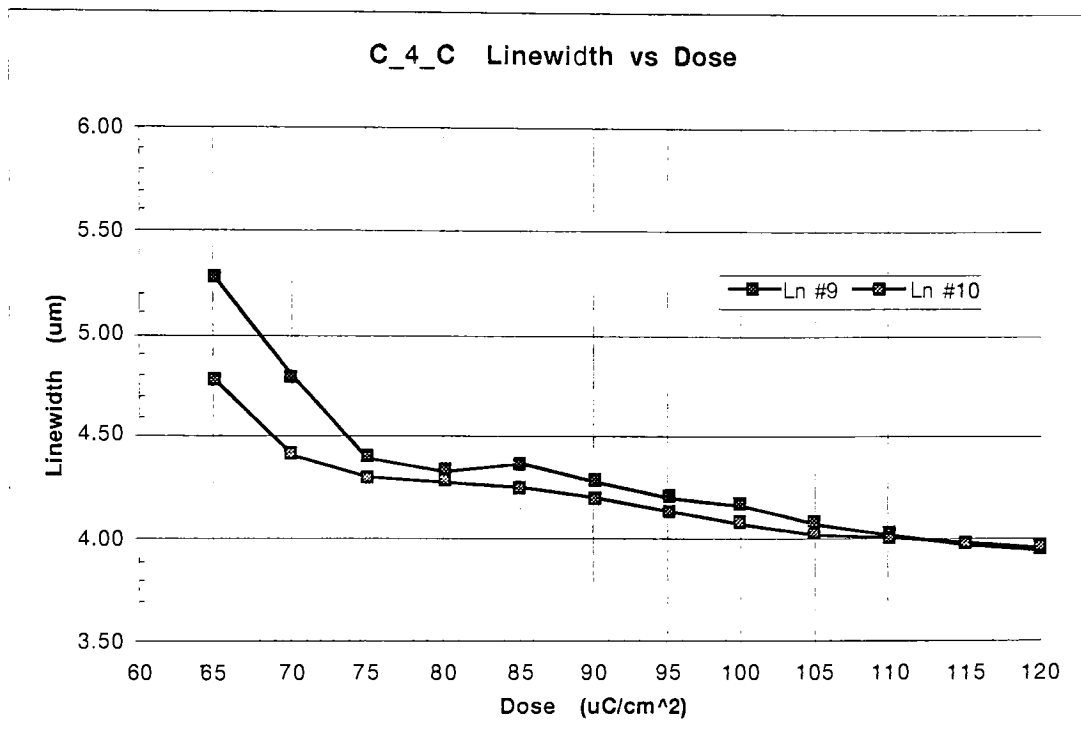
C_4_2 Linewidth vs Dose



Appendix F (Cont.)

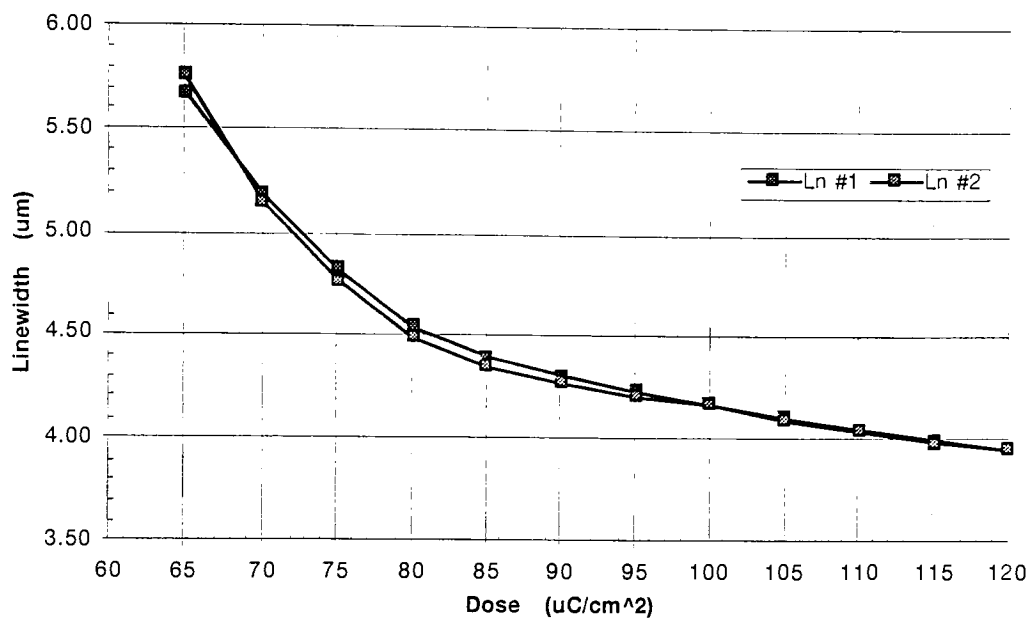


Appendix F (Cont.)

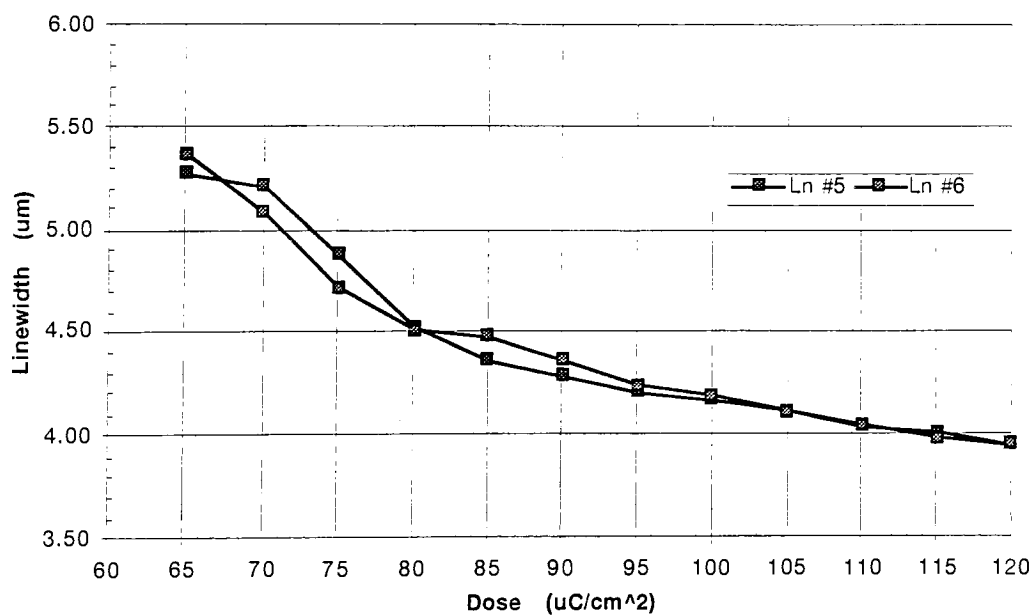


Appendix F (Cont.)

A_6 Linewidth vs Dose



P_6 Linewidth vs Dose



APPENDIX G

Confirmation Runs for Experimental Samples

Appendix G (Cont.)

C 4 - 1

	1	2	3	4	5	6	7	8	9	10	11	12	13	14	15
1	10.47	10.46	10.41	10.37	10.41	10.34	10.34	10.30	10.30	10.31	10.32	10.35	10.34	10.35	10.35
2	10.49	10.45	10.41	10.36	10.41	10.36	10.36	10.30	10.31	10.31	10.35	10.34	10.35	10.35	10.34
3	10.47	10.45	10.40	10.37	10.42	10.35	10.35	10.31	10.31	10.32	10.34	10.33	10.34	10.35	10.35
4	10.47	10.45	10.40	10.37	10.41	10.35	10.35	10.30	10.30	10.32	10.32	10.35	10.35	10.34	10.36
5	10.48	10.44	10.40	10.37	10.41	10.35	10.35	10.32	10.32	10.31	10.34	10.34	10.35	10.36	10.34
6	10.47	10.45	10.42	10.38	10.40	10.33	10.33	10.30	10.32	10.33	10.33	10.35	10.35	10.37	10.34
7	10.49	10.45	10.42	10.35	10.41	10.34	10.34	10.32	10.31	10.30	10.34	10.33	10.34	10.36	10.35
8	10.47	10.44	10.42	10.37	10.41	10.34	10.34	10.30	10.32	10.32	10.34	10.34	10.35	10.35	10.35
9	10.47	10.44	10.40	10.36	10.41	10.35	10.35	10.30	10.32	10.31	10.34	10.35	10.36	10.35	10.34
10	10.47	10.45	10.42	10.37	10.40	10.35	10.35	10.30	10.32	10.31	10.33	10.35	10.35	10.36	10.35

C - 4 - 2

	1	2	3	4	5	6	7	8	9	10	11	12	13	14	15
1	10.69	10.57	10.61	10.64	10.67	10.55	10.54	10.51	10.52	10.51	10.56	10.53	10.55	10.55	10.49
2	10.69	10.57	10.59	10.65	10.66	10.54	10.52	10.50	10.52	10.53	10.57	10.54	10.55	10.54	10.48
3	10.69	10.57	10.60	10.65	10.66	10.54	10.53	10.51	10.53	10.52	10.55	10.55	10.55	10.54	10.47
4	10.70	10.57	10.60	10.62	10.66	10.55	10.51	10.52	10.50	10.53	10.56	10.54	10.55	10.54	10.47
5	10.69	10.56	10.59	10.64	10.67	10.54	10.53	10.52	10.53	10.52	10.56	10.54	10.55	10.54	10.47
6	10.69	10.57	10.59	10.62	10.67	10.55	10.54	10.52	10.52	10.52	10.57	10.54	10.55	10.54	10.50
7	10.69	10.57	10.60	10.64	10.67	10.55	10.54	10.52	10.52	10.54	10.56	10.54	10.55	10.55	10.49
8	10.69	10.57	10.60	10.64	10.67	10.54	10.53	10.51	10.54	10.53	10.56	10.54	10.55	10.54	10.48
9	10.69	10.57	10.61	10.64	10.66	10.55	10.52	10.52	10.52	10.52	10.56	10.54	10.55	10.55	10.48
10	10.69	10.55	10.61	10.64	10.65	10.55	10.53	10.51	10.52	10.51	10.56	10.54	10.56	10.55	10.49

C - 4 - 3

	1	2	3	4	5	6	7	8	9	10	11	12	13	14	15
1	10.69	10.64	10.62	10.61	10.61	10.55	10.54	10.55	10.57	10.51	10.52	10.47	10.49	10.53	10.61
2	10.66	10.63	10.62	10.60	10.61	10.55	10.55	10.57	10.55	10.50	10.52	10.47	10.50	10.51	10.61
3	10.67	10.63	10.63	10.60	10.61	10.55	10.55	10.55	10.56	10.52	10.52	10.48	10.49	10.52	10.61
4	10.67	10.62	10.62	10.60	10.61	10.57	10.54	10.57	10.55	10.52	10.51	10.47	10.49	10.52	10.61
5	10.66	10.64	10.64	10.60	10.61	10.55	10.56	10.55	10.55	10.51	10.50	10.47	10.49	10.52	10.61
6	10.66	10.63	10.62	10.60	10.61	10.56	10.55	10.55	10.55	10.50	10.51	10.49	10.49	10.52	10.61
7	10.66	10.64	10.64	10.61	10.61	10.56	10.55	10.55	10.55	10.51	10.52	10.47	10.49	10.51	10.61
8	10.65	10.64	10.62	10.60	10.61	10.55	10.54	10.55	10.55	10.51	10.52	10.48	10.49	10.52	10.61
9	10.68	10.64	10.64	10.59	10.61	10.55	10.56	10.56	10.55	10.51	10.50	10.48	10.49	10.52	10.61
10	10.67	10.63	10.63	10.61	10.60	10.56	10.54	10.55	10.55	10.50	10.52	10.47	10.49	10.52	10.60

C - 4 - 4

	1	2	3	4	5	6	7	8	9	10	11	12	13	14	15
1	10.62	10.61	10.61	10.61	10.61	10.49	10.52	10.49	10.45	10.52	10.52	10.52	10.49	10.48	10.45
2	10.63	10.61	10.61	10.61	10.61	10.50	10.52	10.49	10.46	10.52	10.51	10.52	10.49	10.49	10.46
3	10.63	10.61	10.62	10.62	10.61	10.50	10.52	10.49	10.45	10.54	10.50	10.51	10.49	10.49	10.45
4	10.63	10.61	10.61	10.62	10.61	10.50	10.51	10.49	10.46	10.51	10.50	10.51	10.49	10.50	10.46
5	10.65	10.62	10.61	10.62	10.61	10.50	10.50	10.49	10.45	10.54	10.52	10.52	10.50	10.48	10.46
6	10.62	10.62	10.61	10.62	10.61	10.50	10.52	10.49	10.46	10.52	10.50	10.51	10.49	10.48	10.45
7	10.64	10.61	10.61	10.61	10.61	10.51	10.50	10.49	10.45	10.50	10.50	10.52	10.49	10.49	10.45
8	10.62	10.62	10.61	10.62	10.61	10.50	10.53	10.49	10.46	10.52	10.51	10.51	10.48	10.49	10.45
9	10.62	10.61	10.62	10.62	10.61	10.51	10.50	10.49	10.46	10.52	10.51	10.51	10.48	10.49	10.45
10	10.63	10.61	10.62	10.61	10.61	10.49	10.50	10.48	10.45	10.51	10.50	10.50	10.49	10.49	10.45

Appendix G (Cont.)

C - 4 - C

	1	2	3	4	5	6	7	8	9	10	11	12	13	14	15
1	11.08	10.93	10.87	10.96	11.04	10.96	10.82	10.84	10.81	10.86	10.92	10.86	10.85	10.81	10.89
2	11.07	10.95	10.87	10.94	11.05	10.94	10.84	10.83	10.82	10.86	10.92	10.84	10.84	10.81	10.88
3	11.08	10.92	10.88	10.95	11.04	10.96	10.84	10.83	10.81	10.85	10.93	10.87	10.83	10.82	10.89
4	11.07	10.93	10.87	10.96	11.04	10.96	10.84	10.84	10.81	10.84	10.93	10.88	10.82	10.82	10.88
5	11.07	10.93	10.89	10.96	11.03	10.96	10.82	10.84	10.81	10.84	10.93	10.86	10.84	10.81	10.89
6	11.06	10.94	10.89	10.96	11.05	10.95	10.84	10.84	10.81	10.85	10.93	10.86	10.84	10.81	10.90
7	11.06	10.92	10.89	10.94	11.04	10.96	10.84	10.84	10.81	10.86	10.93	10.86	10.84	10.82	10.89
8	11.06	10.92	10.89	10.96	11.03	10.95	10.84	10.85	10.82	10.86	10.93	10.87	10.83	10.82	10.88
9	11.07	10.93	10.88	10.96	11.04	10.96	10.84	10.84	10.82	10.86	10.93	10.86	10.83	10.81	10.89
10	11.09	10.92	10.89	10.96	11.03	10.96	10.84	10.83	10.81	10.84	10.93	10.86	10.83	10.81	10.89

A - 6

	1	2	3	4	5	6	7	8	9	10	11	12	13	14	15
1	10.74	10.72	10.71	10.66	10.88	10.84	10.63	10.56	10.58	10.59	10.61	10.59	10.59	10.59	10.56
2	10.74	10.72	10.70	10.89	10.86	10.84	10.61	10.56	10.58	10.59	10.61	10.59	10.60	10.59	10.56
3	10.74	10.71	10.70	10.69	10.67	10.84	10.62	10.57	10.58	10.59	10.61	10.59	10.61	10.58	10.56
4	10.74	10.70	10.70	10.69	10.68	10.65	10.62	10.56	10.60	10.58	10.61	10.60	10.59	10.59	10.55
5	10.74	10.71	10.71	10.89	10.67	10.64	10.61	10.55	10.59	10.59	10.59	10.60	10.61	10.59	10.55
6	10.75	10.71	10.70	10.89	10.67	10.64	10.62	10.55	10.58	10.57	10.60	10.59	10.61	10.59	10.55
7	10.74	10.71	10.70	10.89	10.67	10.65	10.82	10.55	10.59	10.58	10.60	10.59	10.61	10.59	10.55
8	10.74	10.73	10.69	10.89	10.68	10.64	10.61	10.56	10.59	10.58	10.80	10.81	10.59	10.59	10.58
9	10.74	10.71	10.71	10.89	10.66	10.84	10.62	10.56	10.59	10.59	10.60	10.59	10.60	10.59	10.55
10	10.74	10.72	10.70	10.69	10.67	10.85	10.82	10.56	10.59	10.58	10.59	10.60	10.60	10.60	10.55

P - 6

	1	2	3	4	5	6	7	8	9	10	11	12	13	14	15
1	10.81	10.78	10.77	10.78	10.81	10.71	10.68	10.84	10.72	10.73	10.64	10.84	10.59	10.59	10.85
2	10.81	10.76	10.78	10.77	10.79	10.71	10.89	10.65	10.72	10.72	10.64	10.85	10.59	10.59	10.87
3	10.81	10.75	10.77	10.77	10.81	10.72	10.68	10.64	10.71	10.73	10.65	10.64	10.58	10.61	10.88
4	10.83	10.76	10.78	10.78	10.81	10.71	10.68	10.64	10.72	10.72	10.64	10.66	10.59	10.80	10.67
5	10.81	10.76	10.79	10.76	10.81	10.71	10.69	10.64	10.71	10.73	10.65	10.65	10.57	10.60	10.64
6	10.82	10.76	10.77	10.77	10.79	10.72	10.69	10.64	10.72	10.72	10.64	10.65	10.57	10.59	10.66
7	10.81	10.76	10.77	10.77	10.81	10.71	10.89	10.65	10.71	10.72	10.62	10.65	10.59	10.81	10.66
8	10.82	10.76	10.78	10.76	10.81	10.72	10.89	10.66	10.71	10.73	10.66	10.64	10.58	10.59	10.65
9	10.82	10.76	10.77	10.75	10.80	10.71	10.88	10.66	10.72	10.72	10.64	10.65	10.59	10.59	10.67
10	10.82	10.76	10.79	10.76	10.81	10.71	10.68	10.63	10.71	10.73	10.63	10.64	10.57	10.58	10.67